Available online at www.sciencedirect.com
SCIENCE DIRECT®
PERGAMON
Progress in Retinal and Eye Research 22 (2003) 339–358
Progress in
RETINAL AND EYE RESEARCH
www.elsevier.com/locate/prer

In vivo confocal microscopy for evaluation of wound healing following corneal refractive surgery

Timo Tervo*, Jukka Moilanen

Helsinki University Eye Hospital, P.O. Box 220, FIN 00029 HUS, Finland

Abstract

Understanding of corneal wound healing plays an important role, not only in management of corneal infections, but especially in refractive surgery. A better control of wound healing mechanisms might improve the results of such resculpturing techniques and help to avoid complications arising from these procedures. While studies have been focused in different aspects of corneal wound healing, our knowledge has increased greatly during the last years. Many problems associated with corneal healing also contribute to clinical pathology following corneal surgery. Understanding of such conditions has been augmented by the continuously developing corneal imaging techniques. We have used in vivo confocal microscopy (IVCM) for assessing corneas subjected to refractive surgery as well as corneas with common complications resulting from such procedures. IVCM has become a powerful tool for examining corneal cells, nerves, inflammations and infections. It allows information to be acquired repeatedly and at subbiomicroscopic levels that earlier had been obtainable only by invasive microscopic methods. Pre-examining corneas preoperatively by IVCM in order to reveal diseases or conditions in which elective refractive surgical procedures should not be undertaken or to select the ideal operation technique may help to avoid complications in the future. Measurement of the thickness of corneal sublayers or estimation of the thickness of a laser in situ keratomileusis flap or wound bed are other applications in which confocal microscopy may be valuable.

In this article we attempt to describe the in vivo confocal findings of common refractive procedures and their complications, and discuss their biology in light of the existing knowledge on wound healing phenomena.

Keywords: In vivo confocal microscopy; PRK; LASIK; ISCRS; RK; Epikeratophakia; Inflammation; Cornea; Nerves

Contents

*Corresponding author.
E-mail address: timo.tervo@hus.fi (T. Tervo).

1350-9462/03/$ - see front matter
doi:10.1016/S1350-9462(02)00064-2

1. Development of confocal microscopy for clinical research

1.1. History of in vivo imaging of the cornea

The development of the *slit lamp* by Gullstrand (Duke-Elder, 1962) for biomicroscopy of cornea and deeper ocular structures was a major benchmark (Cavanagh et al., 1990, 1993, 1995, 2000; Masters and Farmer, 1993; Masters and Böhnke, 2001, 2002; Petroll et al., 1998) of corneal imaging. The microscope uses a narrow slit to remove part of the scattered light from adjacent tissue structures enabling a degree of optical sectioning, but provides an oblique view and only limited contrast.

Maurice (1974) narrowed the slit and reduced the amount of scattered light to improve the resolution, especially for endothelial cells (*specular microscope*). However, the image was constructed as a photomontage because the tissue was moved against the slit. Koester (1980) introduced a scanning mirror technique to provide a larger field of view ($1\,mm^2$) to image endothelial cells. The slit was now moved against the endothelium. As with the original specular microscope, corneal edema and opacities easily distorted the image, and the microscope had only limited value to image corneal layers other than the endothelium.

1.2. History of in vivo confocal microscopy (IVCM)

The basic idea of IVCM is to minimise scattering of light from structures outside the focal plane enabling optical sectioning of thin layers of the cornea (or other tissues) in order to provide images in x-, y-, z-axes and/or time. These images can be computer manipulated to produce two- or three-dimensional images or numerical data on, e.g. corneal thickness or degree of opacity. While thin (9–40 μm) optical sections are used, opacities in the corneal tissue are less destructive for image formation than with the standard techniques. Confocal microscopes have also become common in microscopy of tissue sections or other specimens in order to provide high contrast for detection of the reaction product in (optically) thin light microscopic sections.

In 1957 Minsky patented the first confocal microscope (Minsky, 1957). In 1968, Petran and Hadravsky developed the tandem scanning confocal microscope (TSCM), which employed the idea of dual light path (for illumination and detection) through a rotating disc. This Nipkow disc contains optically conjugate pinholes arranged densely along Archimedian spirals. The rapid rotation of the disc provided scanning rates suitable for video microscopy. The microscope was adapted for imaging of in vivo cornea by Lemp and co-workers (1985) and later developed by Cavanagh and co-workers (Cavanagh et al., 1990, 1993, 1995, 2000; Jester et al., 1992a; Petrol et al., 1993, 1998). The microscope was equipped with ultraviolet and heath filters (to prevent toxicity from the mercury lamp serving as a light source for the human eye), and applanating objective with motorised drive to enable z-axis scanning. The objective also has "suspension" and alarm to minimise the risk of formation of corneal erosions if the patient moves the eye. The limitations of the technology are its relatively poor light transmission (0.25–2%), and the necessity for an applanating objective, which may cause distorted images. The microscope was approved by FDA and became commercially available as the "Tandem Scanning Confocal Microscope". This particular model is no longer manufactured. Advanced Scanning Corporation now holds the patent rights for future developments.

In contrast, the modified wide field scanning specular microscope described by Koester et al. (1993), with a high numerical aperture objective, can be used for

production of confocal images from all corneal layers on a photography film. The optical section formed is about 40 μm thick rather than 10 μm in the Nipkow-disc-based system. Bright flash and applanating objective are other limitations.

A third design is the *confocal slit microscope* (Masters and Thaer, 1994, 1995). It is a modification of a microscope described by Svischev (1969). The microscope is based on a non-applanating high numerical objective, with two adjustable slits that are used to vary the thickness of the optical section imaged. Scanning and descanning are accomplished by oscillating a two-sided mirror. The scanning images are captured by a CCD camera. The system seems to provide better contrast in some corneal structures, such as wing cells (Masters and Thaer, 1995). This design is now used in clinical models such as in Nidek Confoscan®.

1.2.1. Z-axis measurements and pachymetry features of confocal microscopes

Estimation of the thickness of the various layers of the cornea (epithelium, Bowman's layer, stroma, Descemet's membrane, endothelium) or the thickness of a LASIK flap, wound bed or depth of injury or post-photo refractive keratectomy (PRK) haze is possible with special features and software built in confocal microscopes. To translate the four dimensional (x, y, z, time) information obtainable from living cells and tissues with modern confocal microscopes into numbers, a confocal microscopy through-focusing (CMTF) system was developed by Li and co-workers (1997). The system is based on moving the focal plane rapidly through the entire corneal thickness while producing a stack of 400 two-dimensional images from which a z-axis intensity profile can be calculated by averaging the pixel intensity in the centre of each image and plotting it against z-axis depth. The produced CMTF scan (Fig. 1A) forms intensity peaks from epithelium, subbasal nerve fibre bundles, anterior keratocytes, stromal plateau, and endothelium. The system also quantifies the amount backscattering of light from corneal structures, e.g. such as post-PRK haze (Fig. 1B) or keratocyte activation after laser in situ kertomileusis (LASIK) (Fig. 1C). The unit of measurement (U) is defined as μm × pixel intensity. Finally, the system can be used to create three-dimensional images from the two-dimensional data stacks (Petroll et al., 1993, 1998; Cavanagh et al., 2000; Li et al., 2000). Software for estimation of keratocyte density has also been developed (Mitooka et al., 2002).

Nidek Confoscan® confocal microscope also creates numerical data on the amount of light reflected from each corneal sublayers. This enables measurement of the flap thickness or pachymetry of selected corneal structures. It is also provided with automatic calculating system for corneal endothelial cells. Three-dimensional imaging is also possible with scanning slit confocal microscopes (Masters and Farmer, 1993; Masters and Böhnke, 2001, 2002).

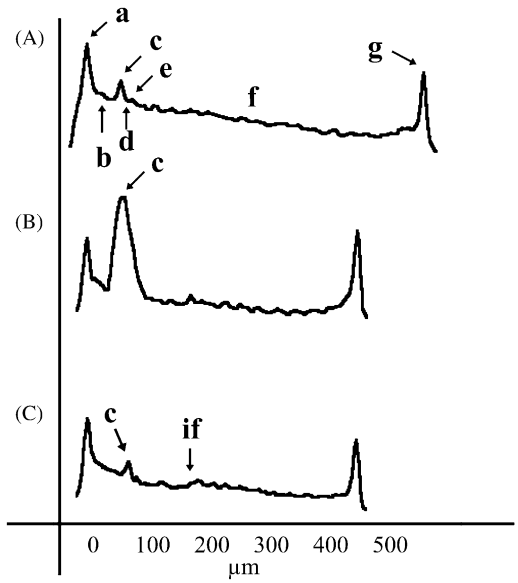

Fig. 1. (A) Normal CMTF intensity profile of the author's cornea (JM). Peaks in the scan correspond to: (a) surface epithelium; (b) basal epithelial cells; (c) subbasal nerve fibre bundles; (d) notch of the non-reflecting Bowman's layer; (e) the most anterior keratocytes; (f) midstromal keratocyte area; (g) endothelium. The height of a peak reflects the intensity (U) of the backscattered light from different sublayers of the cornea. (B) CMTF-scan 3 months after myopic PRK (−3.75 D). The *c*-peak includes the partially regenerated subbasal nerves but most of the intensity of the backscattered light (2321 U) originates from the activated keratocytes and altered extracellular matrix, which constitute the post-PRK the haze. (C) CMTF-scan 3 months after myopic LASIK (−10.0 D, intended flap thickness 180 μm) with only minor keratocyte activity at the interphase area (if; intensity 126 U), measured flap thickness 187 μm.

2. IVCM in corneal research

2.1. Basic parameters of the cornea

Tear film: Prydal and Campbell (1992) have used TSCM to measure the thickness of tear film. However, the applanating objective and use of Goniosol® gel may disturb estimation of tear characteristics.

Epithelium: Irrespective of the type of the microscope, both superficial (Fig. 2A) and basal epithelial cells are easily visualised (Fig. 2B). The impact of limbal stem cell deficiency on corneal healing has also been assessed by IVCM (Cho et al., 1998). Bowman's layer appears as a cell free area, but its thickness (around 16 μm) can be measured using the CMTF feature of TSCM (Cavanagh et al., 2000). Wing cells can probably be imaged with a scanning slit IVCM only (Masters and Thaer, 1995). Subbasal nerve plexus appears as long leashes of branching nerve fibre bundles. The non-reflecting

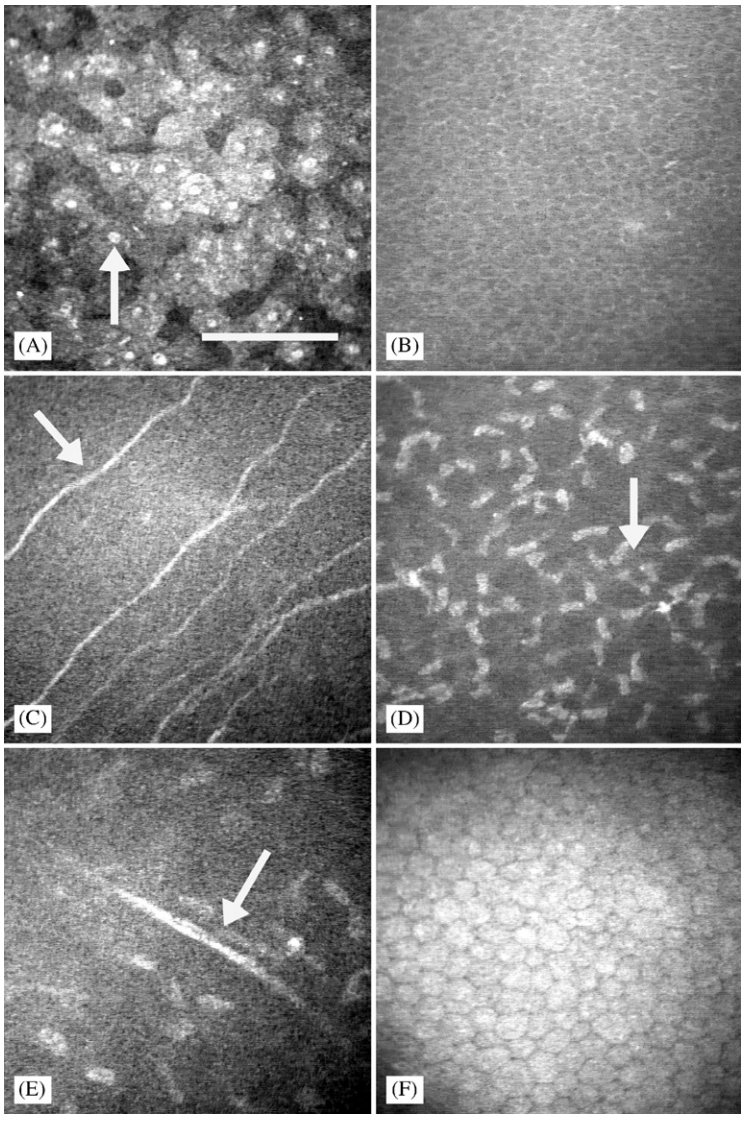

Fig. 2. Normal corneal sublayers imaged by in vivo confocal microscopy: (A) surface epithelium with prominent, bright nuclei (arrow); (B) Basal epithelial cells showing only cell borders; (C) subbasal nerve fibre bundles (arrow); (D) the most anterior keratocytes with bright nuclei, typically forming clusters (arrow); (E) midstromal keratocytes and a stromal nerve (arrow); and (F) endothelium showing mild polymegetism, bar 100 μm.

Bowman's layer rather than the keratocytes is imaged in the same optical section (Fig. 2C).

Stroma: Normal or "quiescent" keratocyte nuclei are easily imaged (Figs. 2D and E) but their processi are only occasionally perceived in healthy corneas. Consequently, confocal microscope is not as accurate as electron microscopy (Muller et al., 1996), histological techniques (Jester et al., 1992a, 1994, 1996, 1997, 1999b; Poole et al., 1993) or laser confocal microscopes (Cavanagh et al., 1995). Alterations in keratocyte phenotype as well as their response to wound healing can also be perceived (Jester et al., 1999a). Collagen laminae are beyond the resolution but in wounded or healing corneas the newly formed extracellular matrix (ECM) can easily be detected (Jester et al., 1999b) and the increased back scattering of light can be translated into numerical values by CMTF (Vesaluoma et al., 2000a; Moilanen et al., 2003; Jester et al., 1999a; Möller Pedersen et al., 1997, 2000; Linna et al., 2000b; Tuominen et al., 2001). Nerves in the mid-stroma are visualised clearly (Fig. 2E).

Stromal cell density in a normal human anterior corneal stroma has been reported to be around 20 000–24 000 cells/mm^3, being highest posterior to the Bowman's layer and then decreasing towards posterior stroma. Keratocyte count decreases with age and seems to be independent upon sex (Erie et al., 1999; Patel et al., 2001a; Berlau et al., 2002). However, Berlau et al. (2002) reported that the density is somewhat higher just anterior to the Descemet's membrane than in the midstroma. *Endothelial cells* (Fig. 2F) and their alterations are usually perceived as with specular microscopes

even in relatively opaque corneas (Koester et al., 1993; Cavanagh et al., 2000; Masters and Thaer, 1994, 1995).

2.2. Corneal infections and inflammations

Confocal microscopy has been used to detect Acanthamoeba cysts (Cavanagh et al., 1993; Mathers et al., 1996, 2000; Pfister et al., 1996; Petroll et al., 1998; Cavanagh et al., 2000). According to our experience, the presence of a cyst is not necessarily an indication to continue the antimicrobial therapy since existence of cysts does not confirm that they are viable (Fig. 3). Fungal (Winchester et al., 1997; Florakis et al., 1997) and bacterial keratitis (Suthpin et al., 1997) can also be assessed by IVCM. Fungal filaments and leukocytes can often be visualised. *Borrelia burgdorferi keratitis* can sometimes be confirmed by confocal microscopy (Linna et al., 1996). Patients with herpetic keratitis show stromal hypercellularity and elongated epithelial cells and activated keratocytes during the early stages (Fig. 4A). Characteristic for the later stages are accumulations of Langerhans-like cells (Fig. 4B) and loss of nerves, which is often patchy after HSV infection and ocular zoster (Böhnke and Masters, 1999; Masters and Böhnke, 2002; Rosenberg et al., 2002).

We recently developed dynamic modification of IVCM in order to image and quantify leukocyte rolling and extravasation in conjuctival venules following inflammatory challenge by cataract surgery (Kirveskari et al., 2001, 2002). This novel non-invasive in vivo technique is based on IVCM using a TSCM microscope of conjunctival venules during inflammation in human patients. In our set up, the inflammation was induced by elective cataract surgery. Only very few, if any rolling or tissue infiltrating leukocytes were found in preoperative analysis. A significant (over 40-fold) increase in the number of rolling cells with a concomitant significant decrease in velocity of the rolling leukocytes was observed at the sites of inflammation. Concomitantly, the number of tissue infiltrating cells was significantly elevated (Fig. 5). When the clinical inflammation resolved, the numbers of rolling and extravasated

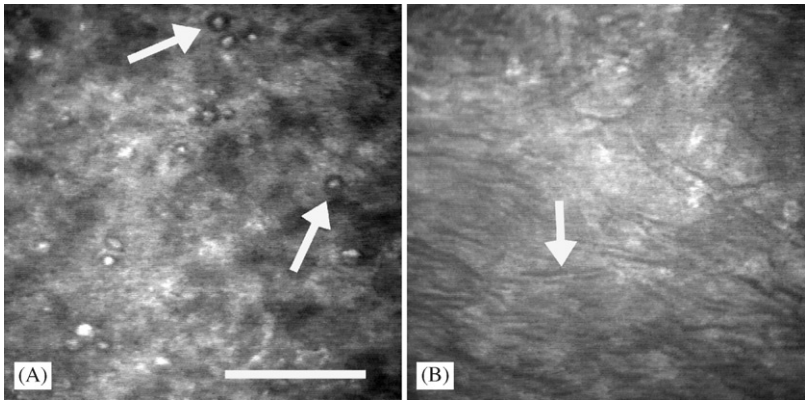

Fig. 3. *Acanthamoeba keratitis*: (A) acanthamoeba cysts present with bright oval particles surrounded by non-reflecting space (arrows) in the surrounding epithelium; and (B) tunnels inside the epithelium (arrow) formed presumably by migration of the protozoa, bar 100 μm.

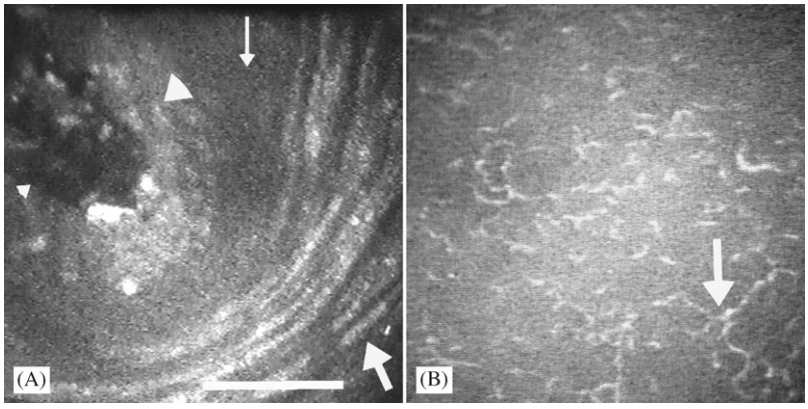

Fig. 4. Herpes simplex-virus (HSV) keratitis: (A) confocal microscopic image of an acute dendritic lesion: the oblique image shows the superficial, elongated epithelial cells (thick arrow), basal epithelial cells (slender arrow), and anterior keratocytes (large arrowhead) encircling the tip of the dendrite (small arrowhead). Bright cells around the lesion may represent active keratocytes and/or inflammatory cells. (B) herpetic lesion in the healing phase. The basal epithelial cell layer still shows dendritic changes (arrow) containing Langerhans-like cells, bar 100 μm.

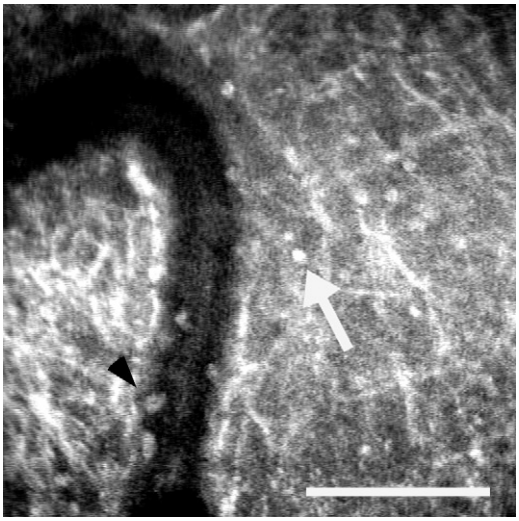

Fig. 5. IVCM image of conjunctival venules adjacent to the wound performed for scleral tunnel in cataract operation. The velocity of the cells inside the vessel is diminished, the cells show rolling (dark arrowhead) and extravasation. During the most prominent inflammation 24 h after the operation extravasated cells can also be seen (white arrow). A week later no signs of inflammation could be observed, bar 100 μm.

leukocytes also decreased back to normal levels (Kirveskari et al., 2001). We have also performed histological biopsies (Kirveskari et al., 2002) from the same areas where the video had been taken and analysed the tissue infiltrated leukocytes from the specimens using immunohistochemistry. Our data suggest that this novel in vivo technique, applicable to human patients in a repeatable manner, will allow the quantitative evaluation of inflammatory conditions or their therapeutic interventions, a task which has previously been approached only invasively. Studies on allergic inflammation and refractive surgery are underway.

3. Refractive surgery

3.1. Radial keratectomy (RK)

RK was the first procedure widely used to alter corneal refractive power. It is based on incision wounds (Jester et al., 1992b), the histology of which has been reviewed in this journal (Jester et al., 1999b). Briefly, an incision wound is first filled by epithelial cells sliding into the wound cleft. Subsequently, these cells form an epithelial plug (at 7 days) that is later replaced by activated keratocytes adapting myofibroblast-like phenotype (at 14 days). These cells accomplish constriction of the wound and form new ECM around the wound thus contributing to scar formation. Similar healing patterns have been observed after performing relaxing incisions or at the edge of the LASIK flap (Linna et al. 2000b; Vesaluoma et al., 2000b). Our IVCM evidence suggests that epithelial cells and microparticles of various origin may persist for years in the wound clefts (Linna et al., 2000b; Vesaluoma et al., 2000b), which may lead to the formation of unstable wounds. Confocal microscopy of such wounds may provide useful clinical information in selected cases of post-RK patients.

3.2. Epikeratophakia

Epikeratophakia is a procedure used mainly during the 1980s and early 1990s for correction of high refractive errors, such as aphakia in children. Certain forms of keratoconus could also be treated. The procedure involves placement of a cryopreserved lenticle from the donor eye in a pocket of the recipient corneal stroma. The epithelium soon covers the acellular graft, which then gets repopulated by stromal cells. The lenticle shows only few, if any, subbasal nerves and normal-looking keratocyte nuclei. Interestingly, some patients show structures resembling nerve bundles or ghost vessels in the interphase between the lenticle and the recipient stroma (Fig. 6).

3.3. Intrastromal corneal ring segments (ISCRS)

Intrastromal corneal ring segments have been approved by FDA for the treatment of myopia from –1 to –3 D and are being studied for the treatment of early keratoconus (Rapuano et al., 2001; Ruckhofer et al., 2001) studied with scanning slit CM eyes with ISCRS, and found a degree of keratocyte activation around the implants. The central cornea, the nerves and the

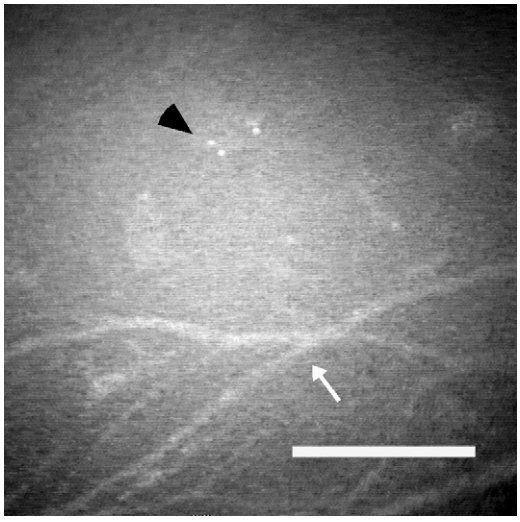

Fig. 6. Confocal microscopic finding of a cornea 10 years after epikeratophakia. The interphase shows branching structures (arrow) that possibly represent stromal nerves or ghost vessels. Persistent bright objects (interphase debris) can also be observed (dark arrowhead), bar 100 μm.

endothelium were normal in all cases. Interestingly, even epithelial cells above the segments showed highly reflective nuclei in areas anterior to the implants.

3.4. Photorefractive keratectomy (PRK)

Reshaping the cornea by a surface photoablation, such as is done in PRK, initiated corneal laser surgery (Trokel et al., 1983). Following epithelial removal by laser or by mechanical- or alcohol-assisted scraping, excimer laser photoablation of the stroma is performed. Thus, epithelium, subbasal nerves, Bowman's layer and variable depth of stromal tissue will be removed. Early investigators often reported relatively long-lasting regression of the induced correction and development of a post-operative anterior stromal scarring or "haze", especially after correction of moderate to high myopia (Frueh et al., 1998; AAO, 1999; Jester et al., 1999b; Möller-Pedersen, 1998a, b, c; Mohan et al., 2003; Moilanen et al., 2003). Improved post-operative management and medication along with newer lasers with smoother or otherwise modified ablation profiles may decrease haze, but no such evidence yet exists.

3.4.1. Wound healing after PRK

Both simple epithelial scrape as well as PRK has been shown to induce death of anterior stromal keratocytes within minutes by apoptosis. Cell death continues for at least a week, but necrosis contributes significantly to death within 24 h of injury (Helena et al., 1998; Mohan et al., 2003). A PRK performed using transepithelial photoablation has been reported to induce less stromal cell apoptosis than PRK performed after surgical scraping of the epithelium (Kim et al., 1998). Even simple epithelial scrape induces keratocyte apoptosis followed by activation of the keratocytes lining the apoptotic zone (Helena et al., 1998; Mohan et al., 2003) but only wounds traversing the Bowman's layer into the stroma induce keratocyte activation followed by long-lasting myofibroblast transformation (Helena et al., 1998; Jester et al., 1999b; Mohan et al., 2003; Fig. 18A). The magnitude of these changes is also related to the amount or depth of photoablation (Möller-Pedersen 1998a, 2000). One explanation could be the progressive neural damage with deeper photoablations. Corneas with neural damage due to any source, such as penetrating keratoplasty (Tuunanen et al., 1997) or disease (AAO, 1999), tend to develop an intense haze and regression following PRK. Compounds typical of active wound healing process such as fibronectin or tenascin initially disappear from subepithelial keratocytes. After repopulation with activated keratocytes (myofibroblasts) there is some overexpression (Van Setten et al., 1992). Stromal cells also exhibit markers for cell proliferation and myofibroblast transformation (Helena et al., 1998; Jester et al., 1999b; Mohan et al., 2003).

3.4.2. Epithelium

IVCM morphology of human cornea during the first days after PRK is poorly understood because of the persistence epithelial defect and the use of bandage contact lenses. Linna and Tervo (1997) observed that the newly healed epithelial cells at day seven show only minor abnormalities. Enlarged epithelial cells have been described in PKP corneas subjected to PRK (Linna and Tervo, 1997). This procedure often produces a strong post-operative haze. Consequently, it is not recommended (Tuunanen et al., 1997). Whether enlarged epithelial cells are typical for corneas with poor sensory innervation remains to be elucidated. Epithelial thickness does not seem to be related to post-PRK regression since post-operative values do not differ from the pre-operative thickness. The method used for epithelial removal had no effect (Möller-Pedersen et al., 2000; Lee et al., 2001).

3.4.3. Stroma

Immediately after PRK, the anterior stromal keratocytes undergo cell death. This is followed by repopulation of the anterior stroma through keratocyte proliferation and infiltration with presumably inflammatory cells (van Setten et al., 1992; Helena et al., 1998; Jester et al., 1999b; Mohan et al., 2003). Migratory, spindle-shaped keratocytes can be observed even with IVCM during the early stages of healing (Jester et al., 1999b). After the repopulation is completed, these cells increase in size, express alpha smooth muscle actin and thus attain the phenotype of myofibroblasts (Jester et al., 1999b; Mohan et al., 2003). The same change occurs in incisional wounds: the wound cleft is first filled with epithelial cells, but by about 14 days migratory keratocytes repopulate the wound edges, migrate into the cleft and subsequently turn into myofibroblast-type cells (Cavanagh et al., 1993; Jester et al., 1999b). Post-PRK keratocyte activation during the first few post-operative weeks is characterised by the presence of prominent cell nuclei, expression of Ki-67 antigen and α-smooth muscle actin and progressive deposition of new ECM (Masur et al., 1996; Linna and Tervo, 1997; Böhnke et al., 1998; Möller-Pedersen et al., 1997, 1998a, b, c; Jester et al., 1999b; Mohan et al., 2003). Activated keratocytes viewed with a confocal microscope also seem to contain small particles (Vesaluoma et al., 2000 a, b). These might represent accumulations of actin filaments (Jester et al., 1999b) (Fig. 7). Keratocyte activation and deposition of new ECM can be observed as early as 7 days post-PRK (Linna and Tervo, 1997) and may persist for years (Moilanen et al., 2003). However, normal-looking keratocytes start to reappear 3–6 months after PRK. Decreased expression of enzyme crystallines in the activated keratocytes has been

proposed to contribute to the increased post-operative backscattering of light (Jester et al., 1999a; Varela et al., 2002).

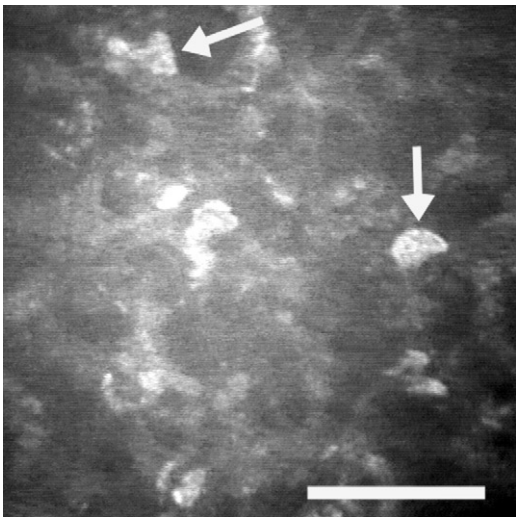

Fig. 7. Anterior stromal keratocytes 2 weeks after hyperopic PRK: cells present with tiny bright, intracellular accumulations (arrows), presumably actin filaments, bar 100 μm.

Studies on both rabbit (Möller-Pedersen et al., 1998c) and human cornea (Möller-Pedersen et al., 2000) have confirmed that true stromal regrowth occurs and can elegantly be shown in three-dimensional images (Fig. 8) (Möller-Pedersen et al., 1998c; Jester et al., 1999b). During the first 2 weeks, four hyperreflective areas can be observed: epithelium, photoablated stromal surface, a layer containing migratory, spindle-shaped keratocytes (Fig. 9) and located under the area of initial stromal cell death, and endothelium. The second and fourth zones merge in about 3 weeks concomitantly with the repopulation of the apoptotic layer in rabbits (Fig. 10). Subsequently, the regrowth continues and may lead to a complete regression of the induced laser surgical correction (Möller-Pedersen et al., 1998b). While rethickening and the amount of the haze in the CMTF scans did not correlate the authors believed that haze formation and stromal regrowth represent separate phenomena. Interestingly, when studying the distribution of α6- and β4-integrins and laminin following PRK, we observed a similar pattern of two gradually merging bands of immunoreactivity, one subepithelially and the other in the anterior stroma (Latvala et al., 1995;

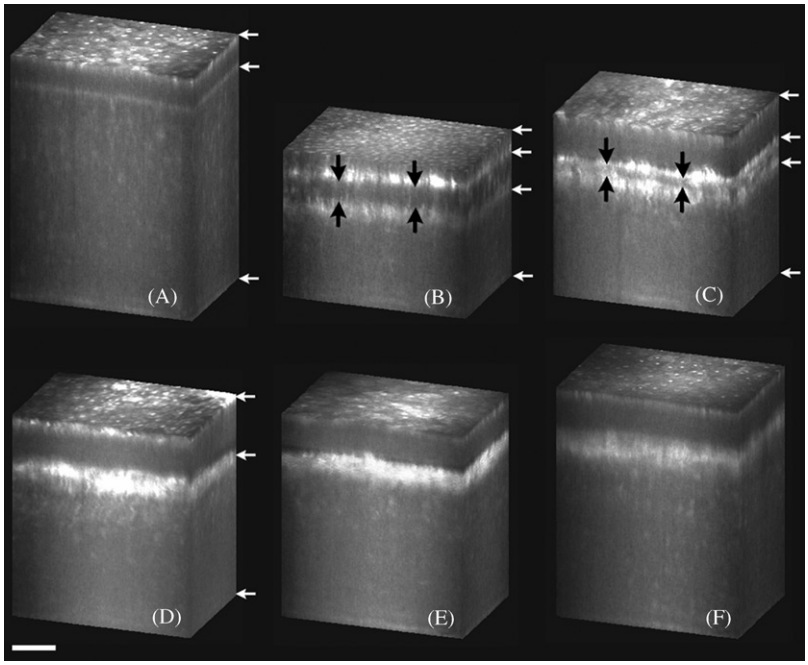

Fig. 8. Three-dimensional reconstructions of IVCM through focusing scans from a rabbit cornea before and after photorefractive keratectomy. In the preoperative cornea (A), three reflective layers were detected corresponding to the superficial epithelium, the epithelial basal lamina, and the endothelium (arrows). 1 week (B) and 2 weeks (C) after PRK, four reflective layers were detected corresponding to the superficial epithelium, the photoablated stromal surface, spindle-shaped fibroblasts, and the endothelium (white arrows). Note that the dark band (black arrows), corresponding to the acellular zone in the anterior stroma, decreases from week one (B) to week two (C). By 3 weeks (D), 7 weeks (E), and 17 weeks (F) after PRK, three reflective layers were detected corresponding to the superficial epithelium, the photoablated stromal surface, and the endothelium (arrows). Note the similarity in the cross-sectional morphology of the photoablated zone with apparent irregularities (B, C, D, F), although the reflectivity seems to decline from week three (D, E, F). Further note that the photoablated zone seems to move up during the study concurrently with a gradually increasing stromal thickness (B, C, D, E, F). bar 100 μm in the *x*-axis and 70 μm in the *z*-axis (voxels are noncubic). The in vivo epithelial and stromal thicknesses were, respectively, (A) 44 and 344 μm, (B) 23 and 216 μm, (C) 58 and 226 μm, (D) 59 and 262 μm, (E) 47 and 272 μm, and (F) 48 and 315 μm. (Taken from Möller-Pedersen et al. (IOVS 39:487-501, 1998) with permission from the Association for Research in Vision and Ophthalmology).

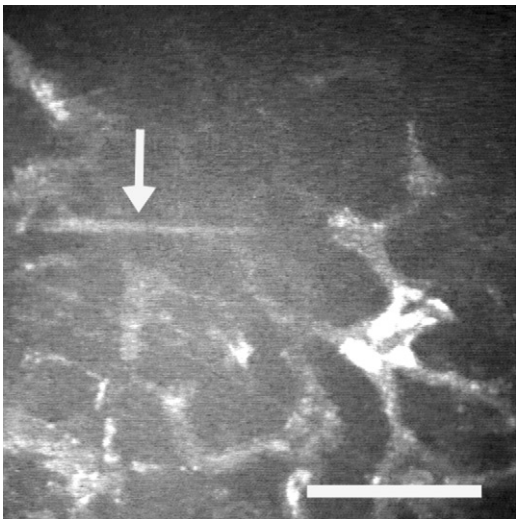

Fig. 9. Anterior stromal keratocytes 1 week after hyperopic PRK: an elongated, spindle-shaped alteration (arrow) probably represents a stromal nerve. Alternatively, it might be a migrating keratocyte described in animal models. Keratocyte activation present as visible processi and brightly reflecting nuclei, bar 100 μm.

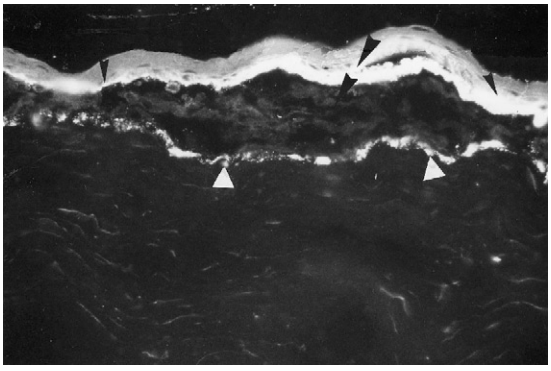

Fig. 10. Immunoreaction for α-6 integrin subunit in the rabbit corneal stroma 2 weeks after PRK. Note that this integrin subunit (as well as another subunit β-4) is located both under the autofluorescent epithelium (black arrowheads) and deeper in the stroma just anterior to the layer of first keratocytes (white arrowheads). α-6/β-4 integrin heterodimer is a component of hemidesmosome. Note also the absence of keratocytes between these two fluorescent lines indicating immunoreaction for α-6 integrin subunit. Immunoreaction for laminin showed identical distribution (data not presented). Compare to Figs. 8 A–F.

Fig. 10). This indicates that the migratory keratocytes express hemidesmosome components and laminin suggesting that they are prepared to establish epithelial attachment structures.

PRK is associated with increased or altered synthesis and release of a number of cytokines in the cornea, tears or lacrimal gland (Li and Tseng, 1995; Tervo et al., 1995; Vesaluoma and Tervo, 1998; Wilson et al., 2001). Cytokines are thought to mediate epithelial–stromal interactions (Li and Tseng, 1995), which induce, e.g. the change in keratocyte phenotype to activated, scar-forming keratocytes. The major candidate cytokines leading to development of fibrosis are TGF-β and PDGF-BB (Möller-Pedersen et al., 1998 a, b; Jester et al., 1999b; Wilson et al., 2001). However, Wilson et al. (2001) reported that tears may not be needed for induction of keratocyte apoptosis. Our own IVCM study revealed that tear fluid TGF-β1 or PDGF-BB or TNF-α levels did not seem to correlate with the density of post-PRK haze evaluated by the CMTF scan (Tuominen et al., 2001).

Rabbit PRK models have shown accumulation of leukocytes in the anterior stroma (Wilson et al., 2001; Mohan et al., 2003). However, IVCM data on the occurrence of inflammatory cells in human post-PRK corneas is scarce—probably due to the fact that studying a human cornea on the first postoperative day must be done either with a contact lens or with a non-contact IVCM. Futhermore, the resolution capacity of the confocal microscope has limitations in distinguishing leucocytes from other cells or fragments of cells (e.g. apoptotic cells). Based on studies with a scanning slit CM, Böhnke and Masters (1999) reported in their review that there was a stromal edema immediately after PRK. They found that an increase of cells in the anterior stroma was demonstrable already on day one. Anterior stromal keratocyte density was elevated up to 4 months. Confirming these findings, Patel and co-workers (1999) reported that on day one after PRK the keratocyte density increased by 9%, and remained elevated for 3 months. Knowing that there should be initial keratocyte death after PRK (Helena et al., 1998; Mohan et al., 2003), these findings might be related to initial appearance of leukocytes and macrophages, followed by keratocyte proliferation and repopulation. However, our own confocal data on inflammatory reaction in conjuctival venules on day one post-PRK have failed to reveal leukocyte rolling. Thus, the situation differs from day one following a cataract operation performed using the phacoemulsification technique (Fig. 5).

3.5. *Laser in situ keratomileusis (LASIK)*

3.5.1. *Epithelium*

Despite the fact that LASIK induces a less pronounced wound healing response (Fig. 1C) (Helena et al., 1998; Peréz-Santonja et al., 1998; Alió et al., 2000; Mohan et al., 2003) and post-operative haze than PRK (Fig. 1B) (El-Maghraby et al., 1999), both the flap and the epithelium may undergo rethickening (Lohman and Guell, 1998; Spadea et al., 2000). An IVCM study recently showed that epithelial thickness increased 22% by 1 month and remained so till 12 months, whereas the thickness of the whole stroma, stromal bed or flap remained virtually unchanged (Erie et al., 2002).

3.5.2. Stroma

Experimental LASIK has been shown to increase keratocyte apoptosis that can be induced within minutes on both sides of the flap (Helena et al., 1998; Wilson et al., 2001; Mohan et al., 2003). Using IVCM for patients who had undergone LASIK, we found "acellular zones" on both sides of the flap interphase (Vesaluoma et al., 2000b). These zones were thickest in corneas investigated 3 days after LASIK, whereas beyond 3 weeks keratocytes appeared in the proximity of both interphases (Fig. 11). However, when compared even with a shallow PRK, LASIK indices far less stromal cell apoptosis and subsequent keratocyte proliferation and transdifferentation to myofibroblasts (Mohan et al., 2003). In human corneas investigated 3 days after LASIK, both highly reflecting oval cells and larger cells with interconnecting prominent processes and some highly reflective extracellular microdots could be observed (Vesaluoma et al., 2000b). Microdots have also been described in corneas subjected to PRK (Böhnke and Masters, 1999). These oval cells may represent large inflammatory cells such as macrophages or a transitional form of keratocyte, and the latter are characteristic for activated keratocytes. After LASIK, the CMTF haze score was highest on day three (earliest time point analysed), and achieved normal levels by 1 month. It correlated with the occurrence of activated keratocytes and formation of new scar-type ECM at the flap interphase rather than number of unidentified debris and particles in the interphase (Vesaluoma et al., 2000b). This cross-sectional study also suggested that the keratocyte density is lower in the flaps than it was preoperatively. The observation was recently confirmed by an IVCM study of Mitooka et al. (2002). They showed that the keratocyte density in the flap decreased from 20% to 40% in the flap and 16% to 30% in the anterior retroablation layer under the flap and remained so at least for 12 months. Keratocyte counts in the deeper stromal layers remained unchanged. This is in agreement with both our data, which showed the keratocyte-free layers on both sides of the flap 3 days after LASIK (Vesaluoma et al., 2000b) and with the experimental data by Helena et al. (1998) and Mohan et al. (2003). The keratocyte-free layers supposedly represent zones undergoing apoptosis/necrosis.

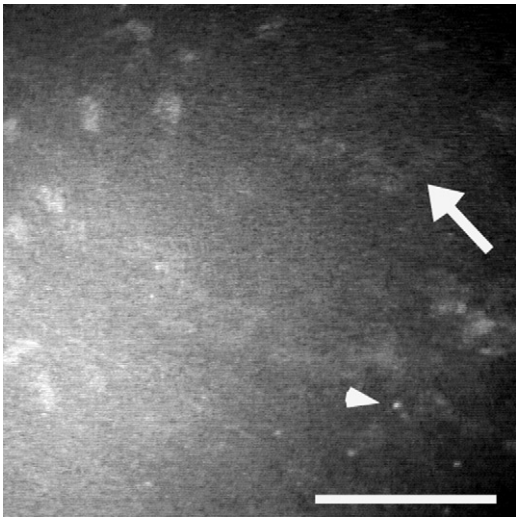

Fig. 11. LASIK interphase 4 weeks post-operatively (−10 D). Mild keratocyte activation immediately under the flap with faint processi (arrow). A few interphase particles are also detectable (arrowhead), bar 100 μm.

3.5.3. Estimation of the flap thickness

The biomechanical strength of the cornea is changed following stromal photoablation. The thickness of the post-LASIK stromal bed is critical when LASIK surgery is planned (Dupps and Roberts, 2001; Mueller et al., 2001; Sugar et al., 2002). Prevention of complications such as post-LASIK keratectasia is thought to require at least 250 μm of stromal bed under the flap (Seiler et al., 1998; Ambrósio and Wilson, 2001; Sugar et al., 2002). Standard pachymetry is routinely used to measure corneal thickness pre-operatively. Different microkeratomes, however, cut flaps with variable precision (Jacobs et al., 1999; Yildirim et al., 2000; Behrens et al., 2000; Gokmen et al., 2002). IVCM provides a precision (resolution 2.6 μm) that is superior to optical coherence tomography for estimation of flap thickness post-operatively (Fig. 1C) (Vesaluoma et al., 2000b; Pisella et al., 2001; Gokmen et al., 2002). We showed that flaps cut with an ACS corneal shaper were thinner than intended (Vesaluoma et al., 2000b). Using the CMTF-scan Gokmen and co-workers (2002) compared two microkeratomes and could show significant difference in their precision: some microkeratomes may also cut thicker flaps than intended. Cases with a thin stromal bed due to overly thick flap cannot be detected by standard pachymetry. Such cases can be detected by IVCM equipped with the CMTF or similar feature.

3.5.4. Wound edge

Wound edge shows normal scar reaction that makes it easily visible under slit lamp. Many of the features in healing of the flap edges resemble what those of linear incision wounds (Jester et al., 1992b, 1999b). While epithelial–stromal interaction (Li and Tseng, 1995; Taliana et al., 2001) is possible at the edge area, there is much more deposition of fibronectin and tenascin at the edges (Peréz-Santonja et al., 1998). Our IVCM observations have revealed that keratocyte activation can regularly be observed at the edges of LASIK wounds. This area may also contain debris. The nerves are cut and, depending upon the quality of apposition, the milieu for neural regeneration may vary (Vesaluoma et al., 2000b).

4. Nerve regeneration after refractive surgery

Both PRK (Campos et al., 1992; Ishikawa et al., 1994; Trabucchi et al., 1994; Kohlhaas et al., 1995; Perez-Santonja et al., 1999; Benitez-del-Castillo et al., 2001) and LASIK (Kanellopoulos et al., 1997; Chuck et al., 2000, Perez-Santonja et al., 1999; Matsui et al., 2001; Linna et al., 2000a; Ang et al., 2001) severe corneal nerves and lead to a loss of corneal sensitivity.

PRK ablates Bowman's layer and the subepithelial nerve plexus. The Bowman's layer shows only minimal if any regeneration after PRK (Moilanen et al., 2003). There is a considerable amount of data on nerve regeneration following PRK: histological sections have revealed presumably regenerating nerve fibres already on day one post-PRK (Tervo et al., 1994; Trabucchi et al., 1994). First regenerating subbasal nerves can be observed at seven days post-PRK using IVCM (Linna and Tervo, 1997). Then a slow increase of fibres and some restoration of subbasal plexus take place. However, histological studies (Tervo et al., 1994) have revealed remarkable long-term morphological alterations and the confocal morphology of the human subbasal plexus is not completely regenerated at 12 months (Linna et al., 2000a). Regeneration extends beyond 12 months, but even after 5 years (Moilanen et al., 2003) some corneas have not reached the normal pattern of innervation (Fig. 12). This agrees well with the histological data by Pallikaris et al. (1990). Unfortunately, the intraepithelial nerves are not usually perceived with IVCM. Consequently, direct comparison of histological and IVCM results is not possible. Furthermore, IVCM does not reveal single regenerating fibres in the stroma. These are visible after both PRK (Tervo et al., 1994) and LASIK (Linna et al., 1998; Trabucchi et al., 1994; Latvala et al., 1996), and show features typical of nerve sprouting. Interestingly, after both PRK (Ishikawa et al., 1994) and LASIK (unpublished observations by the authors), there is an immediate sensory decrease followed by a short period of hypersensitivity 7–9 days after the operation. Subsequently, the mechanical sensitivity seems to recover in about 3–6 months (Campos et al., 1992; Kim and Kim, 1999; Murphy et al., 1999). However, it may be only 50–90% of the preoperative values (Murphy et al., 1999) at 12 months. This is an interesting finding, while activated skin keratinocytes have been shown to synthesise neuronal growth factors (Shu and Mendell, 1999; Hasan et al., 2000; Townley et al., 2002), which in turn induce nerve sprouting and hyperalgesia (Snider and McMahon, 1998; Shu and Mendell, 1999) in experimental models. Furthermore, treatment of animals with capsaicin leads to a decrease in sensitivity followed by nerve sprouting (Fig. 13) (Ogilvy et al., 1991; Marfurt et al., 1993). Using IVCM, we found signs of neural overgrowth in the cornea of a policeman, who was repeatedly exposed to capsaicin-containing tear gas (Vesaluoma et al., 2000c). The cornea also contains a wide variety of neuronal growth factors and their receptors (You et al., 2000). The neuronal system may have an important role during the healing phase after PRK and LASIK. Not only the "sensations of dry eye" reported to be more pronounced after PRK rather than LASIK (Hovanesian et al., 2001), but also the generally known difference in the wound healing response between superficial vs deeper stromal wound models (Jester et al., 1999b; Wilson et al., 2001; Mohan et al., 2003) might result from interference of neural systems in

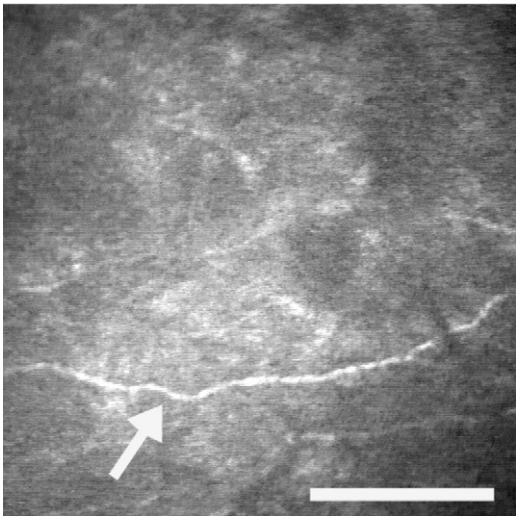

Fig. 12. Recovery of subbasal nerve fibre bundles after myopic PRK. Five years after the operation subbasal nerve plexus is visualised in the same optical section with the anterior keratocytes (arrow). The density of the nerve fibre bundles may not be completely regenerated compared to normal controls (Fig 2C). Excess in the backscattering of light can still be observed. It is mainly derived from ECM. At this stage, the post-PRK haze may be invisible biomicroscopically, bar 100 μm.

Fig. 13. Regenerating nerve fibres in the rabbit corneal stroma 1 month after PRK. Note the numerous regenerating leashes, some which show a growth cone-like ending (arrowheads). Acetylcholinesterase staining.

the healing process. Hyperopic PRK may induce even more profound sensory denervation, since it damages the thick peripheral nerve bundles, thus leading to more profound haze and keratocyte activation in the corneal periphery, as well as in the central area (Fig. 14). Despite the reported regeneration of corneal sensitivity by about 6 months following LASIK, our ongoing studies with a non-contact aesthesiometer have revealed that sensory disturbances may persist up to 2 years. Interestingly, regeneration of subbasal nerves has been reported to correlate with epithelial thickness (Tuominen et al., 2001). Post-LASIK corneas, which have undergone a significant sensory denervation, tend to present with thicker epithelia (Lohman and Guell, 1998). Thus, epithelial hyperplasia is one cause for post-LASIK regression.

LASIK: Stromal and subepithelial nerves are also severed in LASIK, with the exception of those at the flap hinge. Bowman's layer remains intact centrally after LASIK. Consequently, the subbasal nerves retain their topographical environment. Most studies report an early sensory decrease, and recovery during 3–7 post-operative months (Patel et al., 2001b; Chung et al., 2002; Matsui et al., 2001; Linna et al., 2000a). The sensitivity is still subnormal at 6 months after LASIK (Kim and Kim, 1999). However, a correlation between regeneration of subbasal nerve morphology and mechanical sensitivity was observed in an IVCM study by Linna et al. (2000a): First, regenerating fibres appeared as short subbasal leaches. Then by 3 months they were elongated, but interconnections were not observed during the first 6 months (Fig. 15). Interestingly, longitudinal studies done using confocal microscopy (Lee et al., 2002) suggest that morphological recovery of corneal innervation may also take longer than 12 months after LASIK.

Disturbance of the sensory reflex arch between the cornea and lacrimal system may account for the fact that a number of patients display dry eye symptoms or tear fluid abnormalities. Features typical for dry eye, such as lack of the water component and impaired tear fluid stability, have been described (Lee et al., 2000; Yu et al., 2000; Battat et al., 2001; Benitez-del-Castillo et al., 2001; Ang et al., 2001; Toda et al., 2001; Albietz et al., 2002). Impairment of the tear lipid layer has also been reported (Patel et al., 2001b). Consequently, ocular surface disease related to tear fluid abnormalities and/or neurotropic phenomena (Wilson, 2001; Wilson and Ambrosio, 2001) represent the most common adverse effect of LASIK (Fig. 18B) (Sugar et al., 2002; Ambrósio and Wilson, 2001; Wilson and Ambrosio, 2001; Breil et al., 2002). In this respect IVCM can be used to assess post-operative corneas, which show neural damage. IVCM can also be used to differentiate them

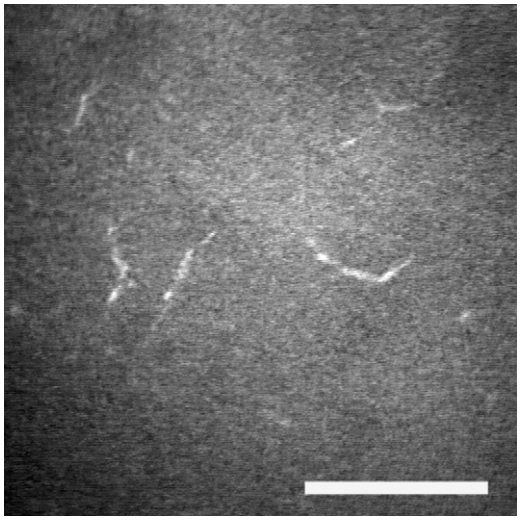

Fig. 15. Short, unconnected subbasal nerve fibre bundles 3 months after LASIK (Taken from Linna et al. (IOVS 41:393-397, 2000) with permission from the Association for Research in Vision and Ophthalmology), bar 100 μm.

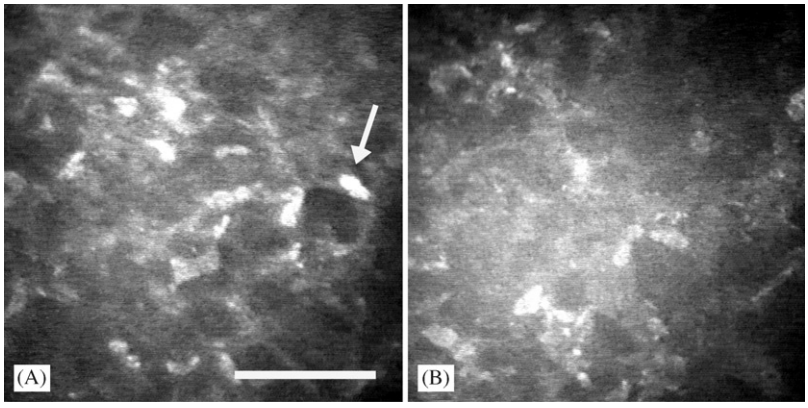

Fig. 14. Keratocyte reaction after hyperopic PRK: (A) Peripheral cornea 2 weeks after the operation shows highly reflecting keratocyte nuclei (arrow) and clearly visible keratocyte processi displaying a honeycomb-like pattern and (B) central cornea 1 week after the operation. Despite of the very shallow photoablation in the central cornea the keratocytes are activated similarly as in the periphery, bar 100 μm.

from eyes with decreased tear secretion, but well regenerated innervation. According to our clinical experience, eyes with impaired sensory innervation should be treated with LASIK rather than PRK because of the high risk for development of stromal haze and regression following the latter procedure. For example, poorly innervated corneal grafts are not suitable for PRK (Tuunanen et al., 1997).

5. Lasik complications

5.1. Interphase debris

Vesaluoma et al. (2000a) showed that there are about 600 (mean) particles per square milllimeter 3 days after LASIK. The particles (Fig. 16A) presumably include cells, cell fragments (apoptotic bodies), debris, metal particles, and salt presipitates from tear film. One month post-operatively the particle count was lower. Improved cleaning procedures adopted after that study seem to have decreased the particle counts. The significance of interphase particles to LASIK complications, such as DLK seems to be minimal.

5.2. Flap striae and folds

Flap striae or macrofolds are indications for lifting the flap as soon as possible after LASIK (Linna et al., 2000b; Ambrósio and Wilson, 2001; Sugar et al., 2002). Large folds can easily be detected under the slit lamp, especially when using retroillumination. Microfolds (Figs. 16B and C) seem to be almost unavoidable (Vesaluoma et al., 2000a), but their impact on visual performance seems to be minimal. They may, however, induce higher-order aberrations existing after flap formation (Pallikaris et al., 2002). Microfolds can occasionally be detected in some other conditions, such as recurrent erosion syndrome (Rosenberg et al., 2000).

5.3. Diffuse lamellar keratitis (DLK)

DLK or "Sands of Sahara" was first discovered by Smith and Maloney (1998) and graded by Linebarger et al. (2000). This condition is characterized by diffuse white, culture-negative keratitis occurring within the first post-operative week (normally on day 1–2) following LASIK.

While the condition seems to be—at least in most cases—sterile (Johnson et al., 2001; Ambrósio and Wilson, 2001) a number of etiologies have been proposed to cause DLK: microkeratome oil (Kaufman et al., 1998), bacterial endotoxins released from sterilizer reservoir biofilms (Holland et al., 2000a) metallic debris from the blade (Kaufman et al., 1998), cleaning solutions (Nakano et al., 2002; Yuhan et al., 2002), carboxymethylcellulose drops (Samuel et al., 2002), Meibomian secretions (Johnson et al., 2001), and activation of endogenous chemotactic systems (Wilson and Ambrósio, 2002). Shah and co-authors (2000), supported by Johnsson et al. (2001), reported a significant association between peroperative epithelial defects and DLK (Fig. 18C). Epithelial defects may also aggravate the risk for development of epithelial ingrowth, as shown in an IVCM study by Sachdev et al. (2002). Johnson et al. (2001) reported an incidence of 1.3% for DLK, but the odds ratio was 13 if any epithelial defect was formed during or immediately after LASIK. While the etiology of DLK has remained unclear some authors have proposed a theory of "multiple factors" (Johnson et al., 2001). A number of studies have revealed accumulations of ovoid cells in the flap interphase (Fig. 16D) at the acute stage followed by some degree of keratocyte activation near the interphase (Vesaluoma et al., 2000a; Buhren et al., 2001; Chung et al., 2002). The ovoid cells have been interpreted to be inflammatory cells, but their size may be too large for granulocytes. Studies done in our laboratory (unpublished), suggest that in case of DLK following an intraoperative epithelial detachment, there is no need for lifting of the flap. The ovoid cells may represent macrophages or some form of keratocytes, which later turn into activated keratocytes (Fig. 16E) (Vesaluoma et al., 2000a; Chung et al., 2002). This interpretation is supported by the fact that neither patients, who develop DLK following an epithelial detachment nor those undergone a normal uneventful LASIK show leukocyte rolling or extravasation in their conjunctival venules (unpublished observations by the authors) as do cataract patients (Kirveskari et al., 2001). However, in our practise the first day post-operative status before removal of the bandage contact lens after LASIK shows marked discharge suggesting the presence of leukocytes on the ocluar surface. We have successfully treated one persistent non-healing post-LASIK epithelial defect with PTK. In case of true flap infection lifting, cleaning, microbial culturing, and immediate antimicrobial therapy is always recommended (Ambrósio and Wilson, 2001; Holland et al., 2000b; Pushker et al., 2002; Sugar et al., 2002). In one case with bacterial through-the flap infection, we lifted the flap, cleaned the interphase and performed PTK on both sides of the hole in the flap and continued the specific antibacterial therapy. The defect had reepithelialized by the following day.

Basement membrane (BM) dystrophy cannot always be excluded clinically. According to our observations (Rosenberg et al., 2001), even asymptomatic (BM) dystrophy eyes can be revealed by IVCM (Fig. 17). Such eyes are probably better candidates for PRK rather than LASIK. Symptomatic post-LASIK BM dystrophy patients can probably be treated with PTK (Rojas and Manche, 2002).

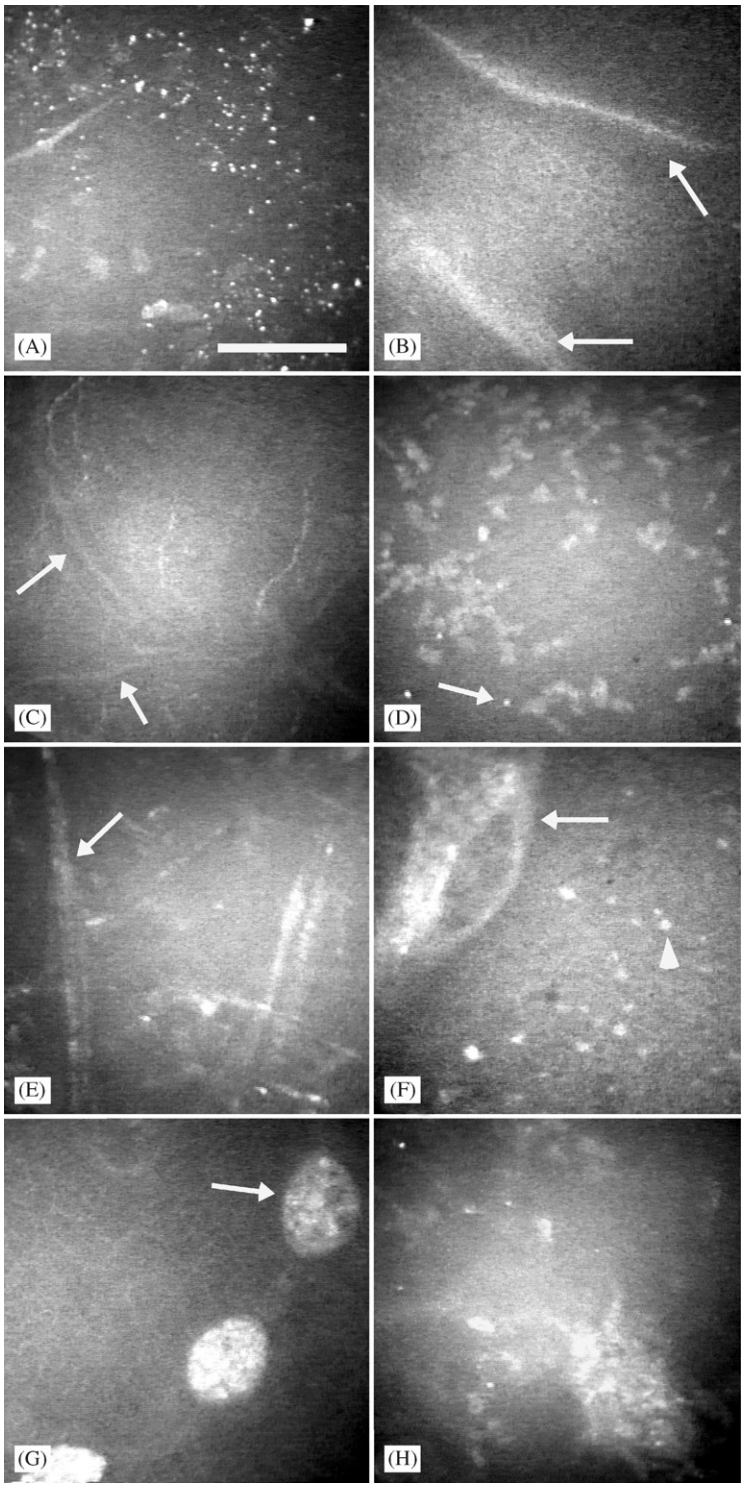

Fig. 16. LASIK-induced complications imaged by IVCM: (A) interphase particles 5 days after the operation; (B) microfolds in the flap 8 days postoperatively: note the two ridges (arrows) in the basal epithelial layer; (C) flap microfolds 3 months post-operatively. Anterior keratocytes, subbasal nerves, and Bowman's layer are located in the same optical section forming detectable ridges (arrows); (D) diffuse lamellar keratitis (DLK), 1 day post-LASIK: the flap interphase area shows accumulation of ovoid objects/cells as well as bright interphase particles (arrow); (E) interphase image 1 week after the onset of late diffuse lamellar keratitis (late DLK) caused by an epithelial defect 8 months after LASIK: post-interphase spindle-shaped elongations (arrow) might represent migratory keratocytes or collagen bundles . No ovoid cells can be detected. The flap was not lifted and cleaned. The patient was treated with systemic and topical steroids; (F) buttonhole of the flap. Scar formation in the wound (arrow) and basal epithelial changes (arrowhead) can be observed at the sites where the blade had excised the epithelium; (G) epithelial ingrowth imaged by IVCM 8 days after the operation. Islands of epithelial cells (arrow) have invaded to the interphase under the flap; and (H) LASIK interphase showing haze formation and accumulation of intralamellar fluid 4 weeks post-operatively. The patient had elevated intraoclular pressure (32 mmHg) and he was a steroid responder, bar 100 μm.

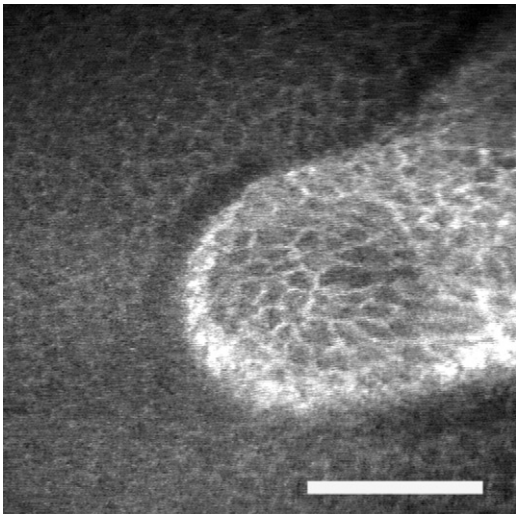

Fig. 17. Confocal microscopic image of a BM dystrophy. Basal epithelial cell layer contains hyperreflective islands of cells. These patients easily develop intraoperative epithelial detachment and subsequently diffuse lamellar keratitis after LASIK, bar 100 μm.

5.4. Button hole

Buttonhole results from a central resurfacing of the microkeratome blade (Johnson et al., 2000; Wilson and Ambrósio, 2001). It is more common in steep corneas (K => 48 D), in which a donut-formed flap may be created. The formation of an epithelial defect allows epithelial–stromal interaction and facilitates scar formation (Li and Tseng, 1995; Wilson et al., 2001). As a result, these corneas show a variable degree of subepithelial haze (Fig. 16F). IVCM can be used to detect cases with buttonhole flaps and differentiate them from very thin central flaps, which also tend to be associated with corneal irregularities and subepithelial haze (Vesaluoma et al., 2000a; Gokmen et al., 2002; Erie et al., 2002.).

5.5. Epithelial ingrowth

Large epithelial cysts (Peréz-Santonja et al., 1998; Alió et al., 2000; Linna et al., 2000b; Vesaluoma et al.,

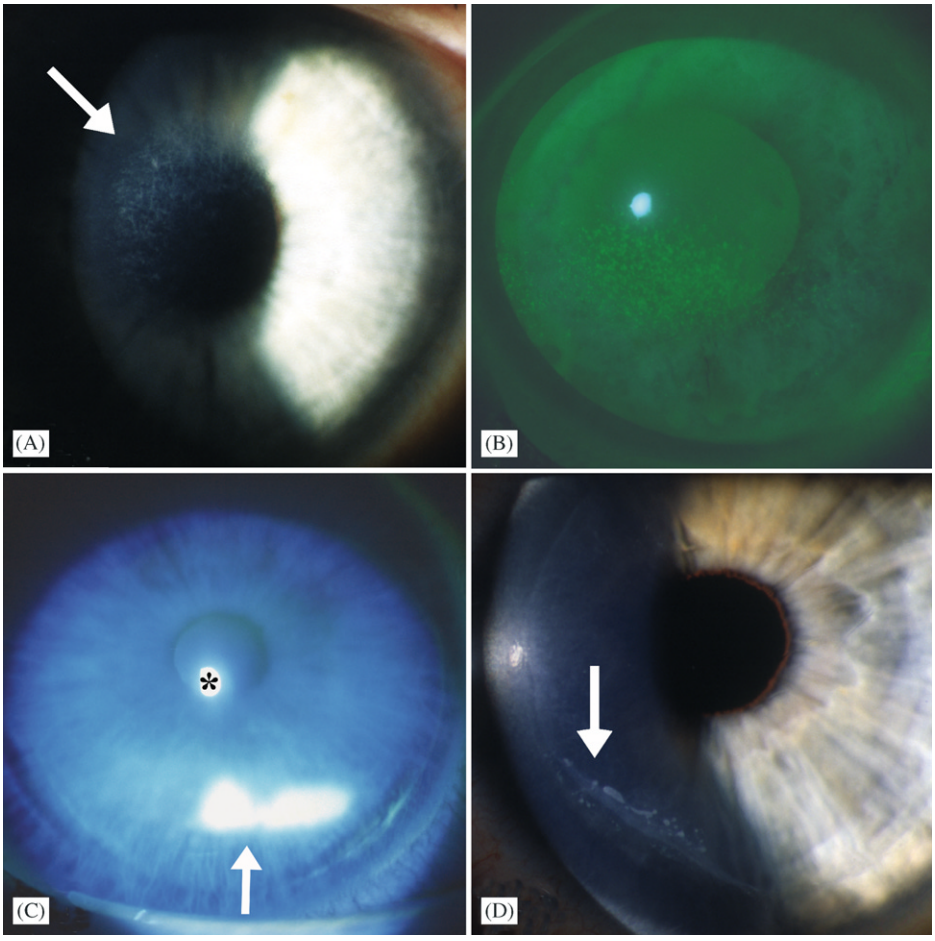

Fig. 18. Anterior segment photographs: (A) subepithelial haze after myopic PRK; (B) presumed LASIK-induced neurotrophic epitheliopathy: damaged superficial epithelial cell staining with fluorescein confined to the flap; (C) epithelial defect after LASIK, stained with fluorescein (arrow). The asterix points at the reflex from the flash light; and (D) epithelial growth within the interphase (arrow) after LASIK (confocal image of the same patient in Fig. 16G).

2000b), visible even with biomicroscopy (Fig. 18D), can easily be imaged with IVCM (Fig. 16G). Similar findings have been found both in RK wounds (Jester et al., 1999b) and relaxing incisions, epithelial cells may persist for months or years in wound clefts (Vesaluoma et al., 2000b). The condition may also lead to flap melt (Alió et al., 2000; Holland et al., 2000; Vesaluoma et al., 2000b), which is a rare complication of LASIK (Wang and Maloney, 2001). It is clinically known that any epithelial tissue under the flap needs to be removed if the melt starts to proceed (Holland et al., 2000; Johnson et al., 2001; Sugar et al., 2002; Ambrósio and Wilson, 2001). Such areas show keratocyte activation, which is probably associated with expression of proteolytic enzyme cascades (Ambrosió and Wilson, 2001). Consequently, IVCM does not offer any additional information that could not be obtained with the slit lamp in this case.

5.6. *Interphase fluid*

Interestingly, the use of topical steroids recommended for the therapy of DLK may cause—if the individual is a steroid responder—elevation of the intraocular pressure (IOP) and accumulation of "interphase fluid" (Lyle and Jin, 1999; Belin et al., 2002) in the stroma. The condition is characterized by regression of the induced refractive result and haze at the flap interphase (Fig. 16H). The underlying condition may also be DLK, but the topical steroids used to treat it may induce elevation of IOP and stromal swelling. Pachymetry or CMTF scans will reveal the diagnosis, as the accumulation of fluid rapidly increases the thickness of the stroma (Belin et al., 2002).

6. Other possibilities in corneal imaging

Means of imaging corneal or other tissues in the eye are being constantly developed. Optical Coherence Tomography (OCT; Humphrey-Zeiss Medical Systems) developed for imaging of retina and optic nerve can also be used for imaging of the cornea and estimation of central corneal thickness (Bechmann et al., 2001; Muscat et al., 2002; Wirbelauer et al., 2002; Neubauer et al., 2002). Nidek EAS-100 anterior segment analysis system also enables imaging of the whole anterior segment including the cornea, as well as objective measurements of tissue opacities such as cataracts (Ito et al., 1999; Vinciquerra et al., 1998). Multi photon confocal microscopy (Masters and So, 1999) has been used for imaging dermal structures, where it seems to offer some benefits over IVCM. Furthermore, a modified IVCM for simultaneous 3D-image formation and CMTF scanning was recently reported (Petroll et al., 2002).

Acknowledgements

Acknowledge is extended to the collaborators and mentors, who have instructed either of the writers into the field of confocal microscopy or corneal refractive surgery or participated in the creation of the results presented. Starting from the beginning, discussions with Stephen Trokel, inventor of PRK and Steven E Wilson, a good friend and prominent scientist in the field of corneal wound healing are to be acknowledged. The authors are also grateful for Professor Wilson for reading and revising of the manuscript. Jorge Alió and Juan Peréz-Santonja helped us in many ways during the early stages, when LASIK was not done in our hospital. Furthermore, help and advice in the field of IVCM by Dwight H Cavanagh, James Jester and Matthew Petroll deserve special recognition. Dr Petroll has been our collaborator (he installed the microscope in our facility). Without his support these studies would not have been possible. Finally, our local Finnish research team: Minna Vesaluoma, Juha Holopainen, Terho Latvala, Tuuli Linna, Maria Rosenberg and Ilpo Tuominen, has worked hard to produce the results and IVCM images. Minna's enthusiasm has inspired our younger investigators tremendously. The ex-Chairman of Helsinki university Eye Hospital, Ahti Tarkkanen has also inspired us all, even after his retirement. Risto Renkonen and Juha Kirveskari, our collaborators in the field immunology and of in vivo confocal imaging of leukocyte rolling and extravasation deserve special appreciation, too.

The financial support (in timely order) by Leiras Medical Manufacturers, Scientific Foundation of Instrumentarium Corp., University of Helsinki, State EVO Grant distributed through Helsinki University Eye Hospital, The Finnish Eye Foundation, and The Eye and Tissue Bank Foundation, Finland has made this study possible.

References

Albietz, J.M., Lenton, L.M., McLennan, S.G., 2002. Effect of laser in situ keratomileusis for hyperopia on tear film and ocular surface. J. Refract. Surg. 18, 113–123.

Alió, J.L., Pérez-Santonja, J.J., Tervo, T., Tabbara, K.F., Vesaluoma, M., Smith, R.J., Maddox, B., Maloney, R.K., 2000. Postoperative inflammation, microbial complications, and wound healing following laser in situ keratomileusis. J. Refract. Surg. 16, 523–538.

Ambrósio Jr., R., Wilson, S.E., 2001. Complications of laser in situ keratomileusis: etiology, prevention, and treatment. J. Refract. Surg. 17, 350–379.

American Academy of Ophthalmology, AAO, 1999. Excimer laser photorefractive keratectomy (PRK) for myopia and astigmatism. Ophthalmology 106, 422–437.

Ang, R.T., Dartt, D.A., Tsubota, K., 2001. Dry eye after refractive surgery. Curr. Opin. Ophthalmol. 12, 318–322.

Battat, L., Macri, A., Dursun, D., Pflugfelder, S.C., 2001. Effects of laser in situ keratomileusis on tear production, clearance, and the ocular surface. Ophthalmology 108, 1230–1235.

Bechmann, M., Thiel, M.J., Neubauer, A.S., Ullrich, S., Ludwig, K., Kenyon, K.R., Ulbig, M.W., 2001. Central corneal thickness measurement with a retinal optical coherence tomography device versus standard ultrasonic pachymetry. Cornea 20, 50–54.

Behrens, A., Langenbucher, A., Kus, M.M., Rummelt, C., Seitz, B., 2000. Experimental evaluation of two current-generation automated microkeratomes: the Hansatome and the Supratome. Am. J. Ophthalmol. 129, 59–67.

Belin, M.W., Hannush, S.B., Yau, C-W., Schultze, R.L., 2002. Elevated intraocular pressure-induced interlamellar stromal keratitis. Ophthalmology 109, 1929–1933.

Benitez-del-Castillo, J.M., del Rio, T., Iradier, T., Hernandez, J.L., Castillo, A., Garcia-Sanchez, J., 2001. Decrease in tear secretion and corneal sensitivity after laser in situ keratomileusis. Cornea 20, 30–32.

Berlau, J., Becker, H-H., Stave, J., Oriwol, C., Guthoff, R., 2002. Depth and age-dependent distribution of keratocytes in healthy human corneas. J. Cataract Refract. Surg. 28, 611–616.

Böhnke, M., Masters, B.R., 1999. Confocal microscopy of the cornea. Prog. Retinal Eye Res. 18, 553–628.

Böhnke, M., Thaer, A., Schipper, I., 1998. Confocal microscopy reveals persisting stromal changes after myopic photorefractive keratectomy in zero haze corneas. Br. J. Ophthalmol. 82, 1393–1400.

Breil, P., Frisch, L., Dick, H.B., 2002. Diagnosis and therapy of LASIK-induced neurotrophic epitheliopathy. Ophthalmologe 99, 53–57.

Buhren, J., Baumeister, M., Kohnen, T., 2001. Diffuse lamellar keratitis after laser in situ keratomileusis imaged by confocal microscopy. Ophthalmology 108, 1075–1081.

Campos, M., Hertzog, L., Garbus, J.J., McDonnell, P.J., 1992. Corneal sensitivity after photorefractive keratectomy. Am. J. Ophthalmol. 114, 51–54.

Cavanagh, H.D., Jester, J.V., Essepian, J., Shields, W., Lemp, M.A., 1990. Confocal microscopy of the living eye. Contact Lens Assoc. Ophthalmol. J. 16, 65–73.

Cavanagh, H.D., Petroll, W.M., Jester, J.V., 1993. The application of confocal microscopy to the study of living systems. Neurosci. Biobehav. Rev. 17, 483–498.

Cavanagh, H.D., Petroll, W.M., Jester, J.V., 1995. Confocal microscopy: uses in measurement of cellular structure and function. Prog. Retinal Eye Res. 14, 527–565.

Cavanagh, H.D., El-Agha, M.S., Petroll, W.M., Jester, J.V., 2000. Specular microscopy, confocal microscopy, and ultrasound biomicroscopy. Cornea 19, 712–722.

Cho, B.-J., Djalilian, A.R., Holland, E.J., 1998. Tandem scanning confocal microscopic analysis of differences between epithelial healing in limbal stem cell deficiency and normal corneal reepithelialization in rabbits. Cornea 17, 68–73.

Chuck, R.S., Quiros, P.A., Perez, A.C., McDonnell, P.J., 2000. Corneal sensation after laser in situ keratomileusis. J. Cataract Refract. Surg. 26, 337–339.

Chung, M.S., Pepose, J.S., Al-Agha, S., Cavanagh, H.D., 2002. Confocal microscopic findings in a case of delayed-onset bilateral diffuse lamellar keratitis after laser in situ keratomileusis. J. Cataract Refract. Surg. 28, 1467–1470.

Duke-Elder, S., 1962. System of Ophthalmology. Kimpton, London, pp. 223–237.

Dupps Jr., W.J., Roberts, C., 2001. Effect of acute biomechanical changes on corneal curvature after photokeratectomy. J. Refract. Surg. 17, 658–669.

El-Maghraby, A., Salah, T., Waring III., G.O., Klyce, S., Ibrahim, O., 1999. Randomized bilateral comparison of excimer laser in situ keratomileusis and photorefractive keratectomy for 2.50 to 8.00 diopters of myopia. Ophthalmology 106, 447–457.

Erie, J.C., Patel, S.V., McLaren, J.W., Maguire, L.J., Ramirez, M., Bourne, W.M., 1999. Keratocyte density in vivo after photorefractive keratectomy in humans. Trans. Am. Ophthalmol. Soc. 97, 221–236.

Erie, J.C., Patel, S.V., McLaren, J.W., Ramirez, M., Hodge, D.O., Maguire, L.J., Bourne, W.M., 2002. Effect of myopic laser in situ keratomileusis on epithelial and stromal thickness. Ophthalmology 109, 1447–1452.

Florakis, G.J., Moazami, G., Schubert, H., Koester, C.J., Auran, J.D., 1997. Scanning slit confocal microscopy of fungal keratitis. Arch. Ophthalmol. 115, 1461–1463.

Frueh, B.E., Cadez, R., Bohnke, M., 1998. In vivo confocal microscopy after photorefractive keratectomy in humans: a prospective, long-term study. Arch. Ophthalmol. 116, 1425–1431.

Gokmen, F., Jester, J.V., Petroll, W.M., McCulley, J.P., Cavanagh, H.D., 2002. In vivo confocal microscopy through-focusing to measure corneal flap thickness after laser in situ keratomileusis. J. Cataract Refract. Surg. 28, 962–970.

Hasan, W., Zhang, R., Liu, M., Warn, J.D., Smith, P.G., 2000. Coordinate expression of NGF and alpha-smooth muscle actin mRNA and protein in cutaneous wound tissue of developing and adult rats. Cell Tissue Res. 300, 97–109.

Helena, M.C., Baerveldt, F., Kim, W.J., Wilson, S.E., 1998. Keratocyte apoptosis after corneal surgery. Invest. Ophthalmol. Vis. Sci. 39, 273–276.

Holland, S.P., Mathias, R.G., Morck, D.W., Chiu, J., Slade, S.G., 2000a. Diffuse lamellar keratitis related to endotoxins released from sterilizer reservoir biofilms. Ophthalmology 107, 1227–1234.

Holland, S.P., Srivannaboon, S., Reinstein, D.Z., 2000b. Avoiding serious corneal complications of laser assisted in situ keratomileusis and photorefractive keratectomy. Ophthalmology 107, 640–652.

Hovanesian, J.A., Shah, S.S., Maloney, R.K., 2001. Symptoms of dry eye and recurrent erosion syndrome after refractive surgery. J. Cataract Refract. Surg. 27, 577–584.

Ishikawa, T., Park, S.B., Cox, C., del Cerro, M., Aquavella, J.V., 1994. Corneal sensation following excimer laser photorefractive keratectomy in humans. J. Refract. Corneal Surg. 10, 417–422.

Ito, Y., Cai, H., Koizumi, Y., Nakao, M., Terao, M., 1999. Correlation between prevention of cataract development by disulfiram and fates of selenium in selenite-treated rats. Curr. Eye Res. 18, 292–299.

Jacobs, B.J., Deutsch, T.A., Rubenstein, J.B., 1999. Reproducibility of corneal flap thickness in LASIK. Ophthalmic Surg. Lasers 30, 350–353.

Jester, J.V., Petroll, W.M., Garana, R.M.R., Lemp, M.A., Cavanagh, H.D., 1992a. Comparison of in vivo and ex vivo cellular structure in rabbit eyes detected by tandem scanning microscopy. J. Microsc. 165, 169–181.

Jester, J.V., Petroll, W.M., Feng, W., Essepian, J., Cavanagh, H.D., 1992b. Radial keratectomy: 1, the wound healing process and measurement of incisional gape in two animal models using in vivo confocal microscopy. Invest. Ophthalmol. Vis. Sci. 33, 3255–3270.

Jester, J.V., Barry, P.A., Lind, G.J., Petroll, W.M., Garana, R., Cavanagh, H.D., 1994. Corneal keratocytes: in situ and in vitro organization of cytoskeletal contractile proteins. Invest. Ophthalmol. Vis. Sci. 35, 730–743.

Jester, J.V., Barry-Lane, P.A., Cavanagh, H.D., Petroll, W.M., 1996. Induction of alpha-smooth muscle actin expression and myofibroblast transformation in cultured corneal keratocytes. Cornea 15, 505–516.

Jester, J.V., Barry-Lane, P.A., Petroll, W.M., Olsen, D.R., Cavanagh, H.D., 1997. Inhibition of corneal fibrosis by topical application of blocking antibodies to TGFbeta in the rabbit. Cornea 16, 177–187.

Jester, J.V., Moller-Pedersen, T., Huang, J., Sax, C.M., Kays, W.T., Cavanagh, H.D., Petrol, W.M., Piatigorsky, J., 1999a. The cellular basis of corneal transparency: evidence for "corneal crystallins". J. Cell Sci. 112, 613–622.

Jester, J.V., Petroll, W.M., Cavanagh, H.D., 1999b. Corneal stromal wound healing in refractive surgery: the role of myofibroblasts. Prog. Retinal Eye Res. 18, 311–356.

Johnson, J.D., Harissi-Dagher, M., Pineda, R., Yoo, S., Azar, D.T., 2001. Diffuse lamellar keratitis: incidence, associations, outcomes, and a new classification system. J. Cataract Refract. Surg. 27, 1560–1566.

Kanellopoulos, A.J., Pallikaris, I.G., Donnenfeld, E.D., Detorakis, S., Koufala, K., Perry, H.D., 1997. Comparison of corneal sensation following photorefractive keratectomy and laser in situ keratomileusis. J. Cataract Refract. Surg. 23, 34–38.

Kaufman, S.C., Maitchouk, D.Y., Chiou, A.G., Beuerman, R.W., 1998. Interphase inflammation after laser in situ keratomileusis. Sands of the Sahara syndrome. J. Cataract Refract. Surg. 24, 1589–1593.

Kim, W.S., Kim, J.S., 1999. Change in corneal sensitivity following laser in situ keratomileusis. J. Cataract Refract. Surg. 25, 368–373.

Kim, W.J., Shah, S., Wilson, S.E., 1998. Differences in keratocyte apoptosis following transepithelial and laser-scrape photorefractive keratectomy in rabbits. J. Refract. Surg. 14, 526–533.

Kirveskari, J., Vesaluoma, M.H., Moilanen, J.A.O., Tervo, T.M.T., Petroll, W.M., Linnolahti, E., Renkonen, R., 2001. A novel non-invasive, in vivo technique for the quantification of leukocyte rolling and extravasation at sites of inflammation in human patients. Nature Med. 7, 376–379.

Kirveskari, J., Helintö, M., Moilanen, J.A.O., Paavonen, T., Tervo, T., Renkonen, R., 2002. Hydrocortisone reduces, in vivo inflammation induced byslow rolling of leukocytes and their extravasation into human conjunctiva. Blood 15, 2203–2207.

Koester, C.J., 1980. Scanning mirror microscope with optical sectioning characteristics: applications to ophthalmology. Appl. Opt. 19, 1749–1757.

Koester, C.J., Auran, J.D., Rosskothen, H.D., Florakis, G.J., 1993. Clinical microscopy of the cornea utilizing optical sectioning and a high-numerical-aperture objective. J. Opt. Soc. Am. A 10, 1670–1679.

Kohlhaas, M., Draeger, J., Lerche, R.C., Klemm, M., Barraquer, C., Barraquer, J.I., Flicker, D., Rivera, F., Carriazo, C., 1995. Corneal reinnervation after keratomileusis in situ and keratomileusis myopica—a comparison. Klin. Monatsbl. Augenheilk. 206, 103–106.

Latvala, T., Tervo, K., Tervo, T., 1995. Reassembly of the $\alpha 6\beta 4$ integrin and laminin in rabbit corneal basement membrane after excimer laser surgery: a 12-month follow-up. Clao. J. 21, 125–129.

Latvala, T., Barraquer-Coll, C., Tervo, K., Tervo, T., 1996. Wound healing and nerve morphology after excimer laser in situ keratomileusis (LASIK) in human eyes. J. Refract. Surg. 12, 677–683.

Lee, J.B., Ryu, C.H., Kim, J., Kim, E.K., Kim, H.B., 2000. Comparison of tear secretion and tear film instability after photorefractive keratectomy and laser in situ keratomileusis. J. Cataract Refract. Surg. 26, 1326–1331.

Lee, Y.G., Chen, W.Y., Petroll, W.M., Cavanagh, H.D., Jester, J.V., 2001. Corneal haze after photorefractive keratectomy using different epithelial removal techniques: mechanical debridement versus laser scrape. Ophthalmology 108, 112–120.

Lee, B.H., McLaren, J.W., Erie, J.C., Hodge, D.O., Bourne, W.M., 2002. Reinnervation in the cornea after LASIK. Invest. Ophthalmol. Vis. Sci. 43, 3660–3664.

Lemp, M.A., Dilly, P.N., Boyde, A., 1985. Tandem scanning confocal microscopy of the full-thickness cornea. Cornea 4, 105–109.

Li, D.Q., Tseng, S.C., 1995. Three patterns of cytokine expression potentially involved in epithelial-fibroblast interactions of human ocular surface. J. Cell. Physiol. 163, 61–79.

Li, H.F., Petroll, W.M., Moller-Pedersen, T., Maurer, J.K., Cavanagh, H.D., Jester, J.V., 1997. Epithelial and corneal thickness measurements by in vivo confocal microscopy through focusing (CMTF). Curr. Eye Res. 16, 214–221.

Li, J., Jester, J.V., Cavanagh, H.D., Black, T.D., Petroll, W.M., 2000. On-line 3-dimensional confocal imaging in vivo. Invest. Ophthalmol. Vis. Sci. 41, 2945–2953.

Linebarger, E.J., Hardten, D.R., Lindstrom, R.L., 2000. Diffuse lamellar keratitis: diagnosis and management. J. Cataract Refract. Surg. 26, 1072–1077.

Linna, T., Tervo, T., 1997. Real-time confocal microscopic observations on human corneal nerves and wound healing after excimer laser photorefractive keratectomy. Curr. Eye Res. 16, 640–649.

Linna, T., Mikkilä, H., Karma, A., Seppälä, I., Petroll, W.M., Tervo, T., 1996. In vivo confocal microscopy: a new possibility to confirm the diagnosis of Borrelial keratitis? (letter). Cornea 15, 639–640.

Linna, T., Peréz-Santonja, J.J., Alió, J., Tervo, T., 1998. Recovery of corneal nerves following laser in situ keratomileusis. Exp. Eye Res. 66, 755–763.

Linna, T., Vesaluoma, M., Pérez-Santonja, J.J., Petroll, W.M., Alió, J., Tervo, T.M.T., 2000a. Effect of myopic LASIK on corneal sensitivity and morphology of subbasal nerves. Invest. Ophthalmol. Vis. Sci. 41, 393–397.

Linna, T., Vesaluoma, M., Petroll, W.M., Tarkkanen, A., Tervo, T., 2000b. Confocal microscopy of a patient with irregular astigmatism after LASIK reoperations and relaxation incisions. Cornea 19, 163–169.

Lohmann, C.P., Guell, J.L., 1998. Regression after lasik for the treatment of myopia: the role of the corneal epithelium. Semin. Ophthalmol. 13, 79–82.

Lyle, W.A., Jin, G.J., 1999. Interphase fluid associated with diffuse lamellar keratitis and epithelial ingrowth after laser in situ keratomileusis. J. Cataract Refract. Surg. 25, 1009–1012.

Marfurt, C.F., Ellis, L.C., Jones, M.A., 1993. Sensory and sympathetic nerve sprouting in the rat cornea following neonatal administration of capsaicin. Somatosens Mot. Res. 10, 377–398.

Masters, B.R., Böhnke, M., 2001. Three-dimensional confocal microscopy of the human cornea in vivo. Ophthalmic. Res. 33, 125–135.

Masters, B.R., Böhnke, M., 2002. Three-dimensional confocal microscopy of the living human eye. Ann. Rev. Biomed. Eng. 4, 69–91.

Masters, B.R., Farmer, M.A., 1993. Three-dimensional confocal microscopy and visualization of the in situ cornea. Comput. Med. Imaging Graphics 17, 211–219.

Masters, B.M., So, P.T.C., 1999. Multi-photon excitation microscopy and confocal microscopy imaging of in vivo human skin, a comparison. Microsc. Microanat. 5, 282–289.

Masters, B.R., Thaer, A.A., 1994. Real-time scanning slit confocal microscopy of the in vivo human cornea. Appl. Optics 33, 695–701.

Masters, B.R., Thaer, A.A., 1995. In vivo real-time confocal microscopy of wing cells in the human cornea: a new benchmark for in vivo corneal microscopy. Bioimages 3, 7–11.

Masur, S., Dewal, H.S., Dinh, T.T., Erenburg, I., Petridou, S., 1996. Myofibroblasts differentiate from fibroblasts when plated at low density. Proc. Natl. Acad. Sci. USA 93, 4219–4223.

Mathers, W.D., Sutphin, J.E., Folberg, R., Meier, P.A., Wenzel, R.P., 1996. Outbreak of keratitis presumed to be caused by Acanthamoeba. Am. J. Ophthalmol. 121, 129–142.

Mathers, W.D., Nelson, S.E., Lane, J.L., Wilson, M.E., Allen, R.C., Folberg, R., 2000. Confirmation of confocal microscopy diagnosis of Acanthamoeba keratitis using polymerase chain reaction analysis. Arc. Ophthalmol. 118, 178–183.

Matsui, H., Kumano, Y., Zushi, I., Yamada, T., Matsui, T., Nishida, T., 2001. Corneal sensation after correction of myopia by

photorefractive keratectomy and laser in situ keratomileusis. J. Cataract Refract. Surg. 27, 370–373.
Maurice, D.M., 1974. A scanning slit optical microscopy. Invest. Ophthalmol. 13, 1033–1037.
Minsky, M., 1957. Memoir on inventing the confocal scanning microscope. J. Scanning 10, 128–138.
Mitooka, K., Ramirez, M., Maguire, L.J., Erie, J.C., Patel, S.V., McLaren, J.V., Hodge, D.O., Bourne, W.M., 2002. Keratocyte density of central human cornea after laser in situ keratomileusis. Am. J. Ophthalmol. 133, 307–314.
Mohan, R.R., Hutcheon, A.E.K., Choi, R., Hong, J.W., Lee, J.S., Mohan, R.R., Ambrosio, R., Zieske, J.D., Wilson, S.E., 2003. Apoptosis, necrosis, proliferation, and myofibroblast generation in the stroma following LASIK and PRK. Experimental Eye Res., in press.
Moilanen, J., Vesaluoma, M., Müller, L., Tervo, T., 2003. Long-term corneal morphology following PRK by in vivo confocal microscopy. Invest. Ophthalmol. Vis. Sci., in press.
Möller-Pedersen, T., Vogel, M., Li, H.F., Petroll, W.M., Cavanagh, H.D., Jester, J.V., 1997. Quantification of stromal thinning, epithelial thickness, and corneal haze after photorefractive keratectomy using in vivo confocal microscopy. Ophthalmology 104, 360–368.
Möller-Pedersen, T., Cavanagh, H.D., Petroll, W.M., Jester, J.V., 1998a. Corneal haze development is regulated by volume of stromal tissue removal. Cornea 17, 627–639.
Möller-Pedersen, T., Cavanagh, H.D., Petroll, W.M., Jester, J.V., 1998b. Neutralizing antibody to TGFbeta modulates stromal fibrosis but not regression of photoablative effect following PRK. Curr. Eye Res. 17, 736–747.
Möller-Pedersen, T., Li, H.F., Petroll, W.M., Cavanagh, H.D., Jester, J.V., 1998c. Confocal microscopic characterization of wound repair after photorefractive keratectomy. Invest. Ophthalmol. Vis. Sci. 39, 487–501.
Möller-Pedersen, T., Cavanagh, H.D., Petroll, W.M., Jester, JV., 2000. Stromal wound healing explains refractive instability and haze development after photorefractive keratectomy: a 1-year confocal microscopic study. Ophthalmology 107, 1235–1245.
Muller, L.J., Pels, L., Vrensen, G.F., 1996. Ultrastructural organization of human corneal nerves. Invest. Ophthalmol. Vis. Sci. 37, 476–488.
Muller, L.J., Pels, E., Vrensen, G.F., 2001. The specific architecture of the anterior stroma accounts for maintenance of corneal curvature. Br. J. Ophthalmol. 85, 437–443.
Murphy, P.J., Corbett, M.C., O'Brart, D.P., Verma, S., Patel, S., Marshall, J., 1999. Loss and recovery of corneal sensitivity following photorefractive keratectomy for myopia. J. Refract Surg. 15, 38–45.
Muscat, S., McKay, N., Parks, S., Kemp, E., Keating, D., 2002. Repeatability and reproducibility of corneal thickness measurements by optical coherence tomography. Invest. Ophthalmol. Vis. Sci. 43, 1791–1795.
Nakano, E.M., Nakano, K., Oliveira, M.C., Portellinha, W., Simonelli, R., Alvarenga, L.S., 2002. Cleaning solutions as a cause of diffuse lamellar keratitis. J. Refract. Surg. 18, S361–363.
Neubauer, A.S., Priglinger, S.G., Thiel, M.J., May, C.A., Welge-Lussen, U.C., 2002. Sterile structural imaging of donor cornea by optical coherence tomography. Cornea 21, 490–494.
Ogilvy, C.S., Silverberg, K.R., Borges, L.F., 1991. Sprouting of corneal sensory fibres in rats treated at birth with capsaicin. Invest. Ophthalmol. Vis. Sci. 32, 112–121.
Pallikaris, I.G., Papatzanaki, M.E., Stathi, E.Z., Frenschock, O., Georgiadis, A., 1990. Laser in situ keratomileusis. Lasers Surg. Med. 10, 463–468.
Pallikaris, I.G., Kymionis, G.D., Panagopoulou, S.I., Siganos, C.S., Theodorakis, M.A., Pallikaris, A.I., 2002. Induced optical aberrations following formation of a laser in situ keratomileusis flap. J. Cataract Refract. Surg. 28, 1737–1741.
Patel, S.V., McLaren, J.W., Camp, J.J., Nelson, L.R., Bourne, W.M., 1999. Automated quantification of keratocyte density by using confocal microscopy in vivo. Invest. Ophthalmol. Vis. Sci. 40, 320–326.
Patel, S.V., McLaren, J.W., Hodge, D.O., Bourne, W.M., 2001a. Normal human keratocyte density and corneal thickness measurement by using confocal microscopy in vivo. Invest. Ophthalmol. Vis. Sci. 42, 333–339.
Patel, S., Pérez-Santonja, J.J., Alió, J.L., Murphy, P.J., 2001b. Corneal sensitivity and some properties of the tear film after laser in situ keratomileusis. J. Refract. Surg. 17, 17–24.
Pérez-Santonja, J.J., Linna, T.U., Tervo, K., Sakala, H.F., Alió Y Santz, J.L., Tervo, T., 1998. Corneal wound healing after laser in situ keratomileusis in rabbits. J. Refract. Surg. 14, 602–609.
Perez-Santonja, J.J., Sakla, H.F., Cardona, C., Chipont, E., Alio, J.L., 1999. Corneal sensitivity after photorefractive keratectomy and laser in situ keratomileusis for low myopia. Am. J. Ophthalmol. 127, 497–504.
Petran, M., Hadravsky, M., Egger, M.D., Galambos, R., 1968. Tandem-scanning reflected-light microscopy. J. Opt. Soc. Am. 58, 661–664.
Petroll, W.M., Cavanagh, H.D., Jester, J.V., 1993. Three-dimensional imaging of corneal cells using in vivo confocal microscopy. J. Microsc. 170, 213–219.
Petroll, W.M., Cavanagh, H.D., Jester, J.V., 1998. Clinical confocal microscopy. Curr. Opin. Ophthalmol. 9, 59–65.
Petroll, W.M., Yu, A., Li, J., Jester, J.V., Cavanagh, H.D., 2002. A prototype two-detector confocal microscope for in vivo corneal imaging. Scanning 24, 163–170.
Pfister, D.R., Cameron, J.D., Krachmer, J.H., Holland, E.J., 1996. Confocal microscopy findings of *Acanthamoeba keratitis*. Am. J. Ophthalmol. 121, 119–128.
Pisella, P.-J., Auzerie, O., Bokobza, Y., Debbasch, C., Baudouin, C., 2001. Evaluation of corneal stromal changes in vivo after laser in situ keratomileusis with confocal microscopy. Ophthalmology 108, 1744–1750.
Poole, C.A., Brookes, N.H., Clover, G.M., 1993. Keratocyte network visualised in the living cornea using vital dyes. J. Cell Sci. 106, 685–692.
Prydal, J.I., Campbell, F.W., 1992. Study of precorneal tear film thickness and structure by interferometry and confocal microscopy. Invest. Ophthalmol. Vis. Sci. 33, 1996–2005.
Pushker, N., Dada, T., Sony, P., Ray, M., Agarwal, T., Vajpayee, R.B., 2002. Microbial keratitis after laser in situ keratomileusis. J. Refract. Surg. 18, 280–286.
Rapuano, C.J., Sugar, A., Koch, D.D., Agapitos, P.J., Culbertson, W.W., de Luise, V.P., Huang, D., Varley, G.A., 2001. Intrastromal corneal ring segments for low myopia: a report by the American Academy of Ophthalmology. Ophthalmology 108, 1922–1928.
Rojas, M.C., Manche, E.E., 2002. Phototherapeutic keratectomy for anterior basement membrane dystrophy after laser in situ keratomileusis. Arch. Ophthalmol. 120, 722–727.
Rosenberg, M.E., Tervo, T.M.T., Petroll, W.M., Vesaluoma, M.H., 2000. In vivo confocal microscopy of patients with corneal recurrent erosion syndrome or epithelial basement membrane dystrophy. Ophthalmology 107, 565–573.
Rosenberg, M.E., Tervo, T.M.T., Mueller, L.J., Moilanen, J.A.O., Vesaluoma, M.H., 2002. In vivo confocal microscopy after herpes keratitis. Cornea 21, 265–269.
Ruckhofer, J., Stoiber, J., Alzner, E., Grabner, G., 2001. Multicenter European Corneal Correction Assessment Study Group one year results of European Multicenter Study of intrastromal corneal ring segments Part 2: complications, visual symptoms, and patient satisfaction. J. Cataract Refract. Surg. 27, 287–296.

Sachdev, N., McGhee, C.N., Craig, J.P., Weed, K.H., McGhee, J.J., 2002. Epithelial defect, diffuse lamellar keratitis, and epithelial ingrowth following post-LASIK epithelial toxicity. J. Cataract Refract. Surg. 28, 1463–1466.

Samuel, M.A., Kaufman, S.C., Ahee, J.A., Wee, C., Bogorad, D., 2002. Diffuse lamellar keratitis associated with carboxymethylcellulose sodium 1% after laser in situ keratomileusis. J. Cataract Refract. Surg. 28, 1409–1411.

Seiler, T., Koufala, K., Richter, G., 1998. Iatrogenic keratectasia after laser in situ keratomileusis. J. Refract. Surg. 14, 312–317.

Shah, M.N., Misra, M., Wihelmus, K.R., Koch, D.D., 2000. Diffuse lamellar keratitis associated with epithelial defects after laser in situ keratomileusis. J. Cataract Refract. Surg. 26, 1312–1318.

Shu, X.Q., Mendell, L.M., 1999. Neurotrophins and hyperalgesia. Proc. Natl. Acad. Sci. USA 96, 7693–7696.

Smith, R.J., Maloney, R.K., 1998. Diffuse lamellar keratitis: a new syndrome in lamellar refractive surgery. Ophthalmology 105, 1721–1726.

Snider, W.D., McMahon, S.B., 1998. Tackling pain at the source: new ideas about nociceptors. Neuron 20, 629–632.

Spadea, L., Fasciani, R., Necozione, S., Balestrazzi, E., 2000. Role of the corneal epithelium in refractive changes following laser in situ keratomileusis for high myopia. J. Refract. Surg. 16, 133–139.

Sugar, A., Rapuano, C.J., Culbertson, W.W., Huang, D., Varley, G.A., Agapitos, P.J., deLuise, V.P., Koch, D.D., 2002. Laser in situ keratomileusis for myopia and astigmatism: safety and efficacy: a report by the American Academy of Ophthalmology. Ophthalmology. 109, 175–187.

Suthpin, J.E., Kantor, A.L., Mathers, W.D., Mehaffey, M.G., 1997. Evaluation of infectious crystalline keratitis with confocal microscopy in a case series. Cornea 16, 21–26.

Svischev, G.M., 1969. Microscope for the study of transparent lighty-scattering objects in incident light. Opt. Spectrosc. 30, 1615–1619.

Taliana, L., Evans, M.D., Dimitrijevich, S.D., Steele, J.G., 2001. The influence of stromal contraction in a wound model system on corneal epithelial stratification. Invest. Ophthalmol. Vis. Sci. 42, 81–89.

Tervo, K., Latvala, T.M., Tervo, T.M., 1994. Recovery of corneal innervation following photorefractive keratoablation. Arch. Ophthalmol. 112, 1466–1470.

Tervo, T., Mertaniemi, P., Vesaluoma, M., 1995. Inflammación en chirurgia refractiva. In: Alio, J., Carreras, B., Ruiz Moreno, J. (Eds.), Inflammaciones oculares. Oficial de la Sociedad Espanola de Oftalmología. 71, 449–461 and 567.

Toda, I., Asano-Kato, N., Komai-Hori, Y., Tsubota, K., 2001. Dry eye after laser in situ keratomileusis. Am. J. Ophthalmol. 132, 1–7.

Townley, S.L., Grimbaldeston, M.A., Ferguson, I., Rush, R.A., Zhang, S.H., Zhou, X.F., Conner, J.M., Finlay-Jones, J.J., Hart, P.H., 2002. Nerve growth factor, neuropeptides, and mast cells in ultraviolet-B-induced systemic suppression of contact hypersensitivity responses in mice. J. Invest. Dermatol. 118, 396–401.

Trabucchi, G., Brancato, R., Verdi, M., Carones, F., Sala, C., 1994. Corneal nerve damage and regeneration after excimer laser photokeratectomy in rabbit eyes. Invest. Ophthalmol. Vis. Sci. 35, 229–235.

Trokel, S.L., Srinivasan, R., Bahren, B., 1983. Excimer laser surgery of the cornea. Am. J. Ophthalmol. 96, 710–715.

Tuominen, I.S., Tervo, T.M., Teppo, A.M., Valle, T.U., Gronhagen-Riska, C., Vesaluoma, M.H., 2001. Human tear fluid PDGF-BB, TNF-alpha and TGF-beta1 vs corneal haze and regeneration of corneal epithelium and subbasal nerve plexus after PRK. Exp. Eye Res. 72, 631–641.

Tuunanen, T., Ruusuvaara, P.J., Uusitalo, R.J., Tervo, T., 1997. Photoastigmatic keratectomy for correction of astigmatism in corneal grafts. Cornea 16, 48–53.

Van Setten, G.B., Koch, J.W., Tervo, K., Lang, G.K., Tervo, T., Naumann, G.O., Kolkmeier, J., Virtanen, I., Tarkkanen, A., 1992. Expression of tenascin and fibronectin in the rabbit cornea after excimer laser surgery. Graefes Arch. Clin. Exp. Ophthalmol. 230, 178–183.

Varela, J.C., Goldstein, M.H., Baker, H.V., Schultz, G.S., 2002. Microarray analysis of gene expression patterns during healing of rat corneas after excimer laser photorefractive keratectomy. Invest. Ophthalmol. Vis. Sci. 43, 1772–1783.

Vesaluoma, M.H., Tervo, T.M.T., 1998. Tenascin and cytokines in tear fluid after PRK. J. Refract. Surg. 14, 437–454.

Vesaluoma, M., Pérez-Santonja, J., Petroll, W.M., Linna, T., Alió, J., Tervo, T., 2000a. Corneal stromal changes induced by myopic lasik. Invest. Ophthalmol. Vis. Sci. 41, 369–376.

Vesaluoma, M.H., Petroll, W.M., Pérez-Santonja, J.J., Valle, T.U., Alió, J.L., Tervo, T.M.T., 2000b. Laser in situ keratomileusis flap margin: wound healing and complications imaged by in vivo confocal microscopy. Am. J. Ophthalmol. 130, 564–573.

Vesaluoma, M., Müller, L., Gallar, J., Lambiase, A., Moilanen, J., Hack, T., Belmonte, C., Tervo, T., 2000c. Effects of oleoresin capsicum pepper spray on human corneal morphology and sensitivity. Invest. Ophthalmol. Vis. Sci. 41, 2138–2147.

Vinciguerra, P., Azzolini, M., Radice, P., Sborgia, M., De Molfetta, V., 1998. A method for examining surface and interphase irregularities after photorefractive keratectomy and laser in situ keratomileusis: predictor of optical and functional outcomes. J. Refract. Surg. 14, S204–206.

Wang, M.Y., Maloney, R.K., 2001. Epithelial ingrowth after laser in situ keratomileusis. Am. J. Ophthalmol. 131, 402–403.

Wilson, S.E., 2001. Laser in situ keratomileusis-induced (presumed) neurotrophic epitheliopathy. Ophthalmology 108, 1082–1087.

Wilson, S.E., Ambrósio Jr., R., 2001. Laser in situ keratomileusis-induced neurotrophic epitheliopathy. Am. J. Ophthalmol. 132, 405–406.

Wilson, S.E., Ambrósio Jr., R., 2002. Sporadic diffuse lamellar keratitis (DLK) following LASIK. Cornea 21, 560–563.

Wilson, S.E., Mohan, R.R., Mohan, R.R., Ambrósio, R., Hong, J., Lee, J., 2001. The corneal wound healing response: cytokine-mediated interaction of the epithelium, stroma, and inflammatory cells. Prog. Retin. Eue. Res. 20, 625–637.

Winchester, K., Mathers, W.D., Sutphin, J.E., 1997. Diagnosis of *Aspergillus* keratitis in vivo with confocal microscopy. Cornea 16, 27–31.

Wirbelauer, C., Winkler, J., Bastian, G.O., Haberle, H., Pham, D.T., 2002. Histopathological correlation of corneal diseases with optical coherence tomography. Graefes Arch. Clin. Exp. Ophthalmol. 240, 727–734.

Yildirim, R., Aras, C., Ozdamar, A., Bahcecioglu, H., Ozkan, S., 2000. Reproducibility of corneal flap thickness in laser in situ keratomileusis using the Hansatome microkeratome. J. Cataract Refract. Surg. 26, 1729–1732.

You, L., Kruse, F.E., Volcker, H.E., 2000. Neurotrophic factors in the human cornea. Invest. Ophthalmol. Vis. Sci. 41, 692–702.

Yu, E.Y., Leung, A., Rao, S., Lam, D.S., 2000. Effect of laser in situ keratomileusis on tear stability. Ophthalmology 12, 2131–2135.

Yuhan, K.R., Nguyen, L., Wachler, B.S., 2002. Role of instrument cleaning and maintenance in the development of diffuse lamellar keratitis. Ophthalmology 109, 400–403.